35

Quantitative X-ray Analysis

CHAPTER PREVIEW

Now you've got an idea of how to acquire XEDS spectra and images from thin foils. You understand what factors limit the useful information they may contain and what false and misleading effects may arise. Also you know how to be very sure that a certain characteristic peak is due to the presence of a certain element and the occasions when you may not be so confident. Having obtained a spectrum or image that is qualitatively interpretable, it turns out to be a remarkably simple procedure to convert that information into quantitative data about the distribution of elements in your specimen; this is what we describe in this chapter.

This chapter is a little longer than the average. You may find that you can skip parts of it as you work through it the first time. We have decided to keep the material together so as to be a more useful reference when you are actually doing your analyses on your microscope. This aspect of XEDS is poised to change significantly in the future and the prospects for much improved quantification are hinted at and covered in detail in the companion text.

35.1 HISTORICAL PERSPECTIVE

Quantitative X-ray analysis in the AEM is a straightforward technique. What is surprising is that, given its simplicity, relatively few users take the trouble to extract quantitative data from their spectra, or produce quantitative images, despite the fact that numerical data are the basis for all scientific investigations. Before we describe the steps for quantification, you should know a little about the historical development of quantitative X-ray analysis, because this will emphasize the advantages of thin-foil analysis over analysis of bulk specimens, which was in fact the driving force for the development of the first commercial analytical TEMs.

Historically, X-ray analysis in electron-beam instruments started with the study of bulk specimens in which the electron beam was totally absorbed, as opposed to 'thin' specimens through which the beam penetrates. The possibility of using X-rays generated by a focused electron beam to give elemental information about the specimen was first described by Hillier and Baker in 1944, and the necessary instrumentation was built several years later by Castaing in 1951. In his extraordinary Ph.D. dissertation, Castaing not only described the equipment but also outlined the essential steps to obtain quantitative data from bulk specimens. The procedures that Castaing proposed still form the basis of the quantification routines used today in the EPMA and may be summarized as follows. Castaing assumed that the concentration C_i of an element i in the specimen generates a certain intensity of characteristic X-rays. However, it is very difficult in practice to measure this generated intensity so Castaing suggested that a known standard of composition $C_{(i)}$ be chosen for element i. We then measure the intensity ratio $I_i/I_{(i)}$

I_i is the measured intensity emerging from (not generated within) the **specimen**.
$I_{(i)}$ is the measured intensity emerging from the **standard**.

Castaing then proposed that, to a reasonable approximation

$$C_i/C_{(i)} = [K]I_i/I_{(i)} \tag{35.1}$$

where K is a sensitivity factor (not a constant) that takes into account the difference between the *generated* and *measured* X-ray intensities for both the standard and the unknown specimen. The contributions to K come from three effects

- Z The atomic number
- A The absorption of X-rays within the specimen
- F The fluorescence of X-rays within the specimen

The correction procedure in bulk analysis is often referred to as the ZAF correction. The necessary calculations, which have been refined over the years since

Castaing first outlined them, are exceedingly complex and best handled by a computer. If you're interested, there are several standard textbooks available which describe the ZAF and related procedures in detail, for example, those by Goldstein et al. and by Reed.

It was soon realized that, if an electron-transparent rather than a bulk specimen was used, the correction procedure could be greatly simplified. To a first approximation, in thin films, the A and F factors could be ignored and only the Z correction would be necessary. Furthermore, in thin specimens, the analysis volume would be substantially reduced, giving a much better spatial resolution. (We discuss this latter point in detail in the next chapter.)

These two obvious advantages of thin-foil analysis led to the development of the so-called Electron Microscope MicroAnalyzer (EMMA), pioneered by Duncumb in England in the 1960s. Unfortunately, the EMMA was far ahead of its time, mainly because the WDS was the only X-ray detector available. As we have seen back in Chapter 32, the classic WDS is handicapped by its poor collection efficiency, relatively cumbersome size, and slow, serial operation. These factors, particularly the poor efficiency, meant that a large probe size (~0.2 μm) had to be used to generate sufficient X-ray counts for quantification of the weak signal from thin foils and, therefore, the gain in spatial resolution over the EPMA was not so great. Also, the poor stability of the WDS meant that it was necessary to measure the beam current to make sure that the X-ray intensities from both standard and unknown could be sensibly compared. As a result of all these drawbacks, the EMMA never sold well and the manufacturer (AEI) soon went out of the EM business.

It is ironic that around this time the commercial developments that would transform TEMs into viable AEMs were all taking place. The XEDS detector was developed in the late 1960s, and commercial TEM/STEM systems appeared in the mid-1970s. However, before the demise of the EMMAs, they were to play a critical role in the development of the thin-foil analysis procedures that, surprisingly, we still use today. The EMMA at the University of Manchester, operated by Graham Cliff and Gordon Lorimer, was re-fitted with an XEDS system and they soon realized that the pseudo-parallel collection mode, the greater collection efficiency, and the improved stability of the XEDS removed many of the problems associated with WDS on the EMMA. Cliff and Lorimer (1975) showed that quantification was possible using a simplification of Castaing's original ratio equation, in which there was no need to incorporate intensity data from a standard, but simply ratio the intensities gathered from two elements simultaneously in the XEDS. This finding revolutionized thin-foil analysis and remains the basis for most quantifications today.

35.2 THE CLIFF-LORIMER RATIO TECHNIQUE

The basis for the Cliff-Lorimer technique is to rewrite equation 35.1 as a ratio of two elements A and B in a binary system. We have to measure the above-background characteristic intensities, I_A and I_B, simultaneously. This is trivial with an XEDS and, therefore, there is no need to measure the counts from a standard

THIN SPECIMENS

We assume that the specimen is thin enough so that we can ignore any absorption or fluorescence. This assumption is called the 'thin-foil criterion.'

The weight percents of each element C_A and C_B can then be related to I_A and I_B thus

$$\frac{C_A}{C_B} = k_{AB}\frac{I_A}{I_B} \tag{35.2}$$

This equation is the Cliff-Lorimer equation and the term k_{AB} is often termed the Cliff-Lorimer factor. As with K in equation 35.1, k_{AB} is a sensitivity factor, not a constant, so don't be fooled by the use of this letter. The k-factor varies according to your TEM/XEDS system and the kV you choose. Because we are ignoring the effects of absorption and fluorescence, k_{AB} is related only to the atomic-number correction factor (Z) in Castaing's original ratio equation. Now to obtain an absolute value for C_A and C_B, we need a second equation and, in a binary system, we simply assume that A and B constitute 100% of the specimen, so

$$C_A + C_B = 100\% \tag{35.3}$$

We can easily extend these equations to ternary and higher order systems by writing extra equations of the form

$$\frac{C_B}{C_C} = k_{BC}\frac{I_B}{I_C} \tag{35.4}$$

$$C_A + C_B + C_C = 100\% \tag{35.5}$$

You should also note that the k-factors for different pairs of elements AB, BC, etc., are related thus

$$k_{AB} = \frac{k_{AC}}{k_{BC}} \tag{35.6}$$

So long as you are consistent, you could define the composition in terms of atomic %, or weight fraction or any appropriate units. Of course the value of the k-factor would change accordingly.

Remember that Cliff and Lorimer developed the ratio approach to overcome the limitations of early

AEMs, particularly the low brightness of thermionic sources, the small collection angle of early detectors, electrical and mechanical instabilities (particularly the beam current), and the tendency of the early AEMs to contaminate the analysis area. Consequently, X-ray count rates were very low, thus limiting quantification. So it was very difficult to use the well-established, pure-element standards approach developed over the preceding 25 years for the EPMA because you'd have to keep changing specimens to measure the standards. In doing so, the probe current would change because, in a TEM, you have to switch off the beam to stop the vacuum changes burning out the gun (unlike in an EPMA where you can measure the current in situ and also isolate the gun automatically). Switching the gun on and off prevents any meaningful comparison of standards and unknowns. The ratio approach cancels out variations in the probe current incident on the analysis area; such variations arise from electron-gun/condenser-system instabilities, drift, and contamination buildup. Despite the fact that most of these problems have been minimized in modern AEMs, the ratio technique still remains the only quantitative thin-film analysis software available on commercial XEDS systems. Clearly, this is not an ideal situation and after describing the Cliff-Lorimer method, we'll discuss the ζ-factor, an alternative, improved approach, which combines the ease of application of the ratio method with the more rigorous aspects of pure-element (or other) thin-film standards (more about this in the companion text). The ζ-factor method requires in-situ measurement of the probe current, which, while standard on EPMAs for almost 50 years, has still not penetrated the design of commercial AEMs! So, despite its vintage, the Cliff-Lorimer equation remains the basis for quantitative analysis on all AEMs. Let's see how we use it in practice.

WT%

The convention is: define the units of composition as wt%.

35.3 PRACTICAL STEPS FOR QUANTIFICATION

First of all, you should try to use K_α lines, where possible, for the measured counts (I). (The K_β peak is combined with the K_α if the two K peaks cannot be resolved.) Use of L or M lines is more difficult because of the many overlapping lines in each family, but may be unavoidable if the K_α lines are too energetic and go right through your detector. (Think why you can't use L or M lines if the K lines are too *weak* for your detector.)

To gather characteristic X-ray intensities for quantification

- Keep your specimen as close to 0° tilt as possible to minimize spurious effects.
- If you have a wedge specimen, orient it so the thin portion of the wedge faces the detector, to minimize X-ray absorption (see Section 35.6).
- If the area of interest in your specimen is close to a strong two-beam dynamical diffraction condition, tilt it slightly to kinematical conditions.
- Accumulate enough counts in the characteristic peaks, I_A, I_B, etc. As we will see below, for acceptable errors, there should ideally be at least 10^4 counts above background in each peak.

While you can't always obtain 10^4 counts in a reasonable time before specimen drift, damage, or contamination limits your analysis, you should always choose the largest probe size which is consistent with maintaining the desired spatial resolution, so you get most current into your specimen. (Remember all the other ways to maximize the X-ray count rate that we discussed in Chapter 34.)

(The reason we worry a little about the diffraction conditions is that anomalous X-ray generation can occur across bend contours or whenever a diffracted beam is strongly excited. This point is not too critical because we quantify using a ratio technique. If the beam has a large convergence angle, which is usually the case, any diffraction effect is further reduced. However, we will see in Section 35.9 that, under certain conditions, there are some advantages to be gained from such crystallographic effects.)

Having accumulated a spectrum under these conditions, how do you quantify it? All you have to do is measure the peak intensities I_A, I_B, etc., and then determine a value for the k_{AB} factor. To determine the peak intensities, you first have to remove the background counts from the spectrum and then integrate the peak counts. Both of these steps are accomplished by various software routines in the XEDS computer system or in DTSA. There are advantages and disadvantages to each approach, so you should pick the one that is most suited to your problem.

35.3.A Background Subtraction

Remember, as we saw back in Section 4.2.B, we are not very precise in the terminology we use for the X-ray background intensity, so it can be confusing. 'Background' refers to the counts under the characteristic peaks in the spectrum displayed on your computer screen. These X-rays are generated by the 'bremsstrahlung' or 'braking-radiation' process as the beam electrons interact with the coulomb field of the nuclei in the specimen. The intensity distribution of the bremsstrahlung decreases continuously as the X-ray energy increases, reaching zero at the beam energy (go back

and look a, Figure 4.6). Thus, the energy distribution can be described as a 'continuum,' although as we've seen, the phenomenon of coherent bremsstrahlung disturbs this continuum.

TERMINOLOGY

We tend to use these three terms 'background,' 'bremsstrahlung,' and 'continuum' interchangeably, although strictly speaking they have these specific meanings.

Remember also that the generated bremsstrahlung intensity is modified at energies below about 1.5 keV by absorption within the specimen and the detector, so we are usually dealing with a background in the spectrum that looks something like Figure 35.1. The best approach to background subtraction depends on two factors

- whether the region of interest in your spectrum is in the low-energy regime, where the intensity decreases rapidly with decreasing energy.
- if the characteristic peaks you want to measure are close together or isolated.

Window methods: In the simplest case of isolated characteristic peaks superimposed on a slowly varying background, you can easily remove the background counts by drawing a straight line below the peak, and defining the background intensity as that present below the line, as shown in Figure 35.2. So you get the computer first to define a 'window' in the spectrum spanning the width of the peak, and then draw the line between

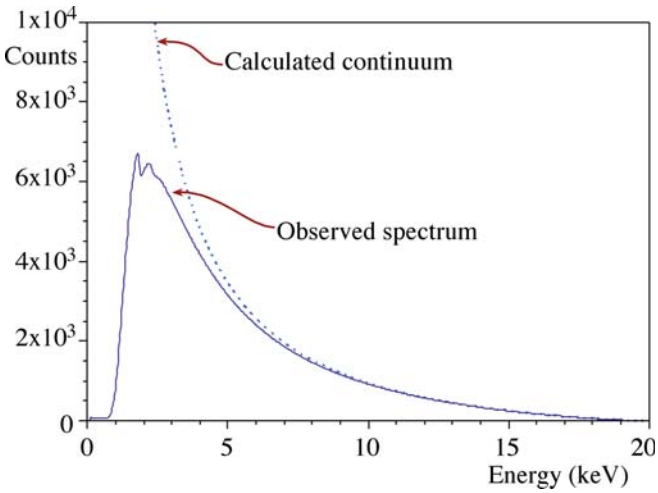

FIGURE 35.1. The theoretically calculated and experimentally observed bremsstrahlung intensity distribution as a function of energy. Both curves are similar until energies below ~2 keV when absorption within the specimen and the XEDS system reduces the detected counts. The best method of background removal depends on where in the spectrum your characteristic peaks are present.

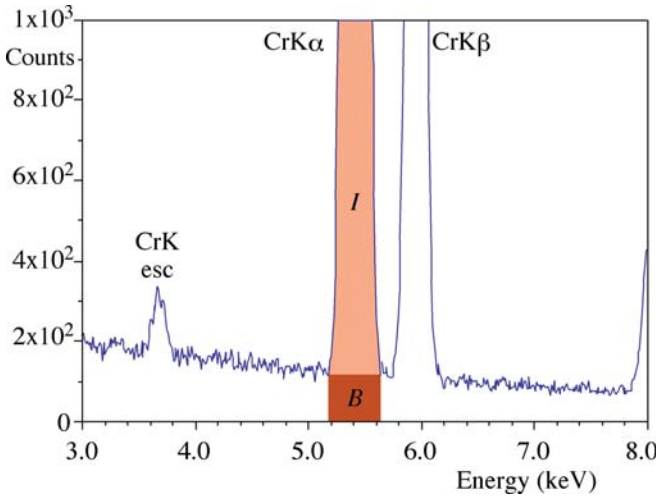

FIGURE 35.2. The simplest method of estimating the background contribution (B) to the counts in the characteristic peak (I); a straight line drawn beneath the Cr K_α peak provides a good estimate, if the counting statistics are good and the intensity approximates to a slowly varying function of energy. There should be no overlap with any other characteristic peak and the peak energy should be > ~2 keV.

the background intensities in the channels just outside the window. As with *all* spectral manipulations, this method gives better results with more counts in the spectrum. The background intensity variation is then less noisy, so it is easier to decide where the peak ends and the background begins and, furthermore, the background variation better approximates to a straight line.

Another, similarly primitive, approach involves averaging the bremsstrahlung counts above and below the characteristic peak by integrating the counts in two identical windows on either side of the peak, as shown in Figure 35.3. We then assume that the average of the two intensities equals the background counts under the

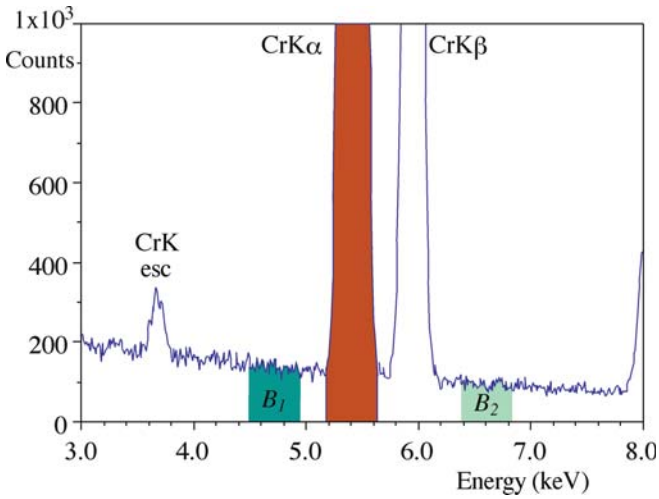

FIGURE 35.3. Background subtraction can be achieved by averaging the bremsstrahlung counts in two identical windows (B_1, B_2) on either side of the characteristic (Cr K_α and K_β) peaks. There should be no overlap with any other characteristic peaks and the peak energy should be >2 keV.

peak. This assumption is reasonable in the higher-energy regions of the spectrum and when the specimen is thin enough so that the bremsstrahlung is not absorbed in the specimen. This absorption happens because the bremsstrahlung X-rays with energies just above the peak energy preferentially fluoresce the characteristic-peak X-rays, resulting in a detectable reduction in the bremsstrahlung counts above the peak energy compared to below.

TOO THICK?

If you see this bremsstrahlung absorption effect in your spectrum, your specimen is too thick for Cliff-Lorimer quantification.

When you use the two-window approach, you must remember the window width you used, because *identical* windows must be used when subtracting the background both in the unknown spectrum and in the spectrum from the known specimen that you will use to determine the *k*-factor (see Section 35.4).

While the two techniques we just described have the advantage of simplicity, you can't always apply them to real specimens because the spectral peaks may overlap. Also, if the peaks lie in the low-energy region of the spectrum where the background is changing rapidly due to absorption, then neither of these two simple methods gives a good estimate of the background and more sophisticated mathematical approaches are required. We'll now discuss these methods.

Modeling the background: the bremsstrahlung distribution can be mathematically modeled, based on the expression developed by Kramers (1923). The number (N_E) of bremsstrahlung photons of energy E produced in a given time by a given electron beam is given by Kramers' law.

$$N_E = KZ\frac{(E_0 - E)}{E} \tag{35.7}$$

Here Z is the *average* atomic number of the specimen, E_0 is the beam energy in keV, and E is the X-ray energy in keV. The factor K in Kramers' law actually takes account of numerous parameters. These include

- Kramers' original constant.
- The collection efficiency of the *detector*.
- The processing efficiency of the *detector*.
- The absorption of X-rays within the *specimen*.

OPTIMUM WINDOW

The typical choice of window width is FWHM, but this throws away a substantial amount of the counts in the peak. FWTM gives better statistics, but incorporates more bremsstrahlung than characteristic counts; 1.2(FWHM) is the optimum window.

All these terms have to be factored into the computer calculation when you use this method of background modeling.

Be wary when using this approach because Kramers developed his law for bulk specimens. However, the expression is still used in commercial software, and seems to do a reasonable job.

Modeling the spectrum produces a smooth curve fit that describes the shape of the complete spectrum. This approach is particularly valuable if many characteristic peaks are present, since then it is difficult to make local measurements of the background counts by a window method. Figure 35.4 shows an example of a spectrum containing many adjacent peaks, with the background counts estimated underneath all the peaks.

Filtering out the background: another mathematical approach to removing the background uses digital filtering. This process makes no attempt to take into account the physics of X-ray production and detection as in Kramers' law. Rather it relies on the fact that the characteristic peaks show a rapid variation of counts as a function of energy (i.e., dI/dE is large), while the background exhibits a relatively small dI/dE. This approximation is valid even in the region of the spectrum below ~ 1.5 keV where absorption is strong. In the process of digital filtering, the spectrum intensity is filtered by convoluting it with another mathematical function. The most common function used is a 'top-hat' filter function, so called because of its shape. When the top-hat filter is convoluted with the shape of a typical X-ray spectrum, it acts to produce a second-difference spectrum, i.e. d^2I/dE^2 versus E. After the top-hat filter, the background with small dI/dE is transformed to a linear

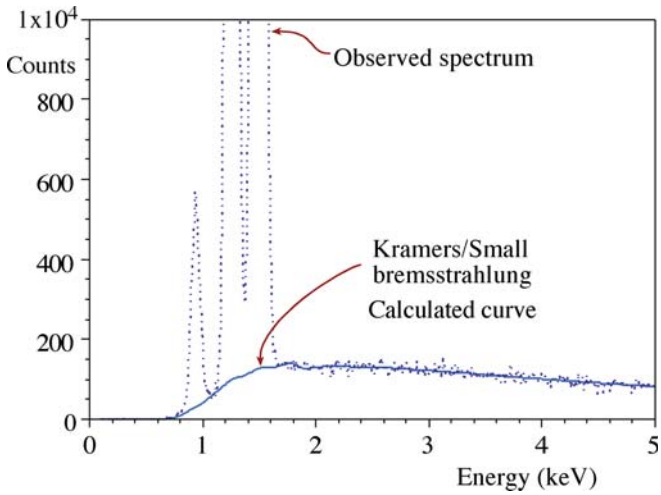

FIGURE 35.4. The bremsstrahlung intensity modeled using Kramers' law, modified by Small to include the effects of absorption of low-energy X-rays in the specimen and the detector. This method is useful when the spectrum contains many overlapping peaks, particularly in the low-energy range, such as the Cu L_α and the Mg and Al K_α lines shown in this spectrum (based on Chapter 34, can you determine which peak is which?).

function with a value of zero (thus it is 'removed'), while the peaks with large dI/dE, although distorted to show negative intensities in some regions, are essentially unchanged as far as the counting statistics are concerned. Figure 35.5A shows schematically the principle behind the filtering process and Figure 35.5B,C shows an example of a spectrum before and after digital filtering.

BACKGROUND REMOVAL

You must always take care to apply the same background-removal process to both the standard and the unknown.

In summary, you can remove the background by selecting appropriate windows to estimate the counts in the peak, or use one of two mathematical-modeling approaches. The window method is generally good enough if the peaks are isolated and on a linear portion of the background. The mathematical approaches are most useful for multi-element spectra and/or those containing peaks below ~1.5 keV. You should choose the method that gives you the most reproducible results (check this on a specimen for which you know the composition).

After removing the background, you have to integrate the peak intensities I_A, I_B, etc.

35.3.B Peak Integration

If you used a window method of background estimation, then the peak counts are obtained simply by subtracting the estimated background counts from the total counts in the chosen window. Therefore, if the computer drew a line under the peak as in Figure 35.2 then the peak intensity is that above the line.

- If you chose, e.g., an ideal window of 1.2 FWHM and averaged the background on either side of the peak then the average value must be subtracted from the total counts in the 1.2 FWHM window; always use the same window width for B and I.

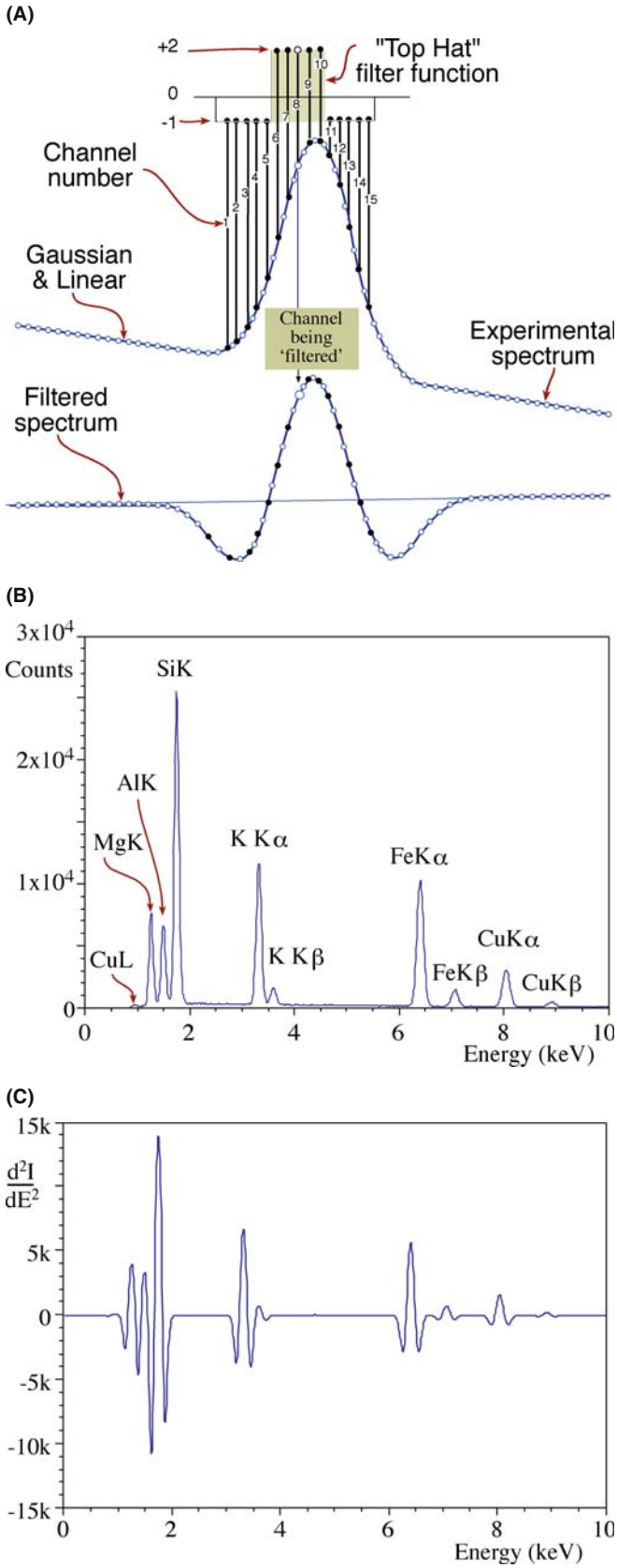

FIGURE 35.5. (A) Digital filtering involves convolution of a top-hat filter function with the acquired spectrum. To obtain the filtered spectrum, each channel has the top-hat filter applied to it. The channels on either side of that being filtered (#8 in this case) are multiplied by the appropriate number in the top-hat function. So channels 1–5 and 11–15 are multiplied by –1 and channels 6–10 by +2. The sum of the multiplications is divided by the total number of channels (15) and allotted to channel #8 in the filtered spectrum at the bottom. The digital filtering process in (A) applied to a spectrum from biotite (B) results in the filtered spectrum (C) in which the background intensity is zero at all places, and the characteristic peaks remain effectively unchanged.

- If you used a Kramers' law fit, the usual method of peak integration is to get the computer to fit the peak with a slightly modified Gaussian, and integrate the total counts in the channels under the Gaussian.
- If a digital filter was used, you have to compare the peaks with those that were taken previously from standards, digitally filtered, and stored in a library in the computer. The library peaks are matched to the experimental peaks via a multiple least-squares fitting procedure and the counts determined through calculation of the fitting parameters.

Each of the two curve-matching processes is rapid. Each can be used to deconvolute overlapping peaks and each uses all the counts in the peak. The Kramers-law fit and the digital filter have much wider applicability than the simple window methods. However, these computer processes are not invariably the best, nor are they without error.

The Gaussian curve fitting must be flexible enough to take into account several variables

- The peak width can change as a function of energy or as a function of count rate.
- The peak distortion due to incomplete charge collection can vary.
- There may be an absorption edge under the characteristic peak if your specimen is too thick.

The creation of a library of spectra gathered under conditions that match those liable to be encountered during analysis (particularly similar count rates and dead times) is a tedious exercise. However, you do get a figure of merit for the 'goodness of fit' between the unknown spectrum and the standard. Usually, a χ^2 value is given which has no absolute significance, but is a most useful diagnostic tool. Typically, the χ^2 value should be close to unity for a good fit, although a higher value may merely indicate that some unidentified peaks were not accounted for during the matching process. What you have to watch out for is a sudden increase in χ^2 compared with previous values. This indicates that something has changed from your previous analyses. Perhaps your standard is not giving a good fit to the experimental spectrum and either a new library spectrum needs to be gathered or the experimental peak should be looked at carefully. For example, another small peak may be hidden under the major peak and would need to be deconvoluted from the major peak before integration proceeds. If you suspect a poor fit, you should make the computer display the 'residuals,' that is the counts remaining in the spectrum after the peak has been integrated and removed. As shown in Figure 35.6, you can easily see if a good fit was made (Figure 35.6A) or if the library peak and the experimental peak do not match well (Figure 35.6B).

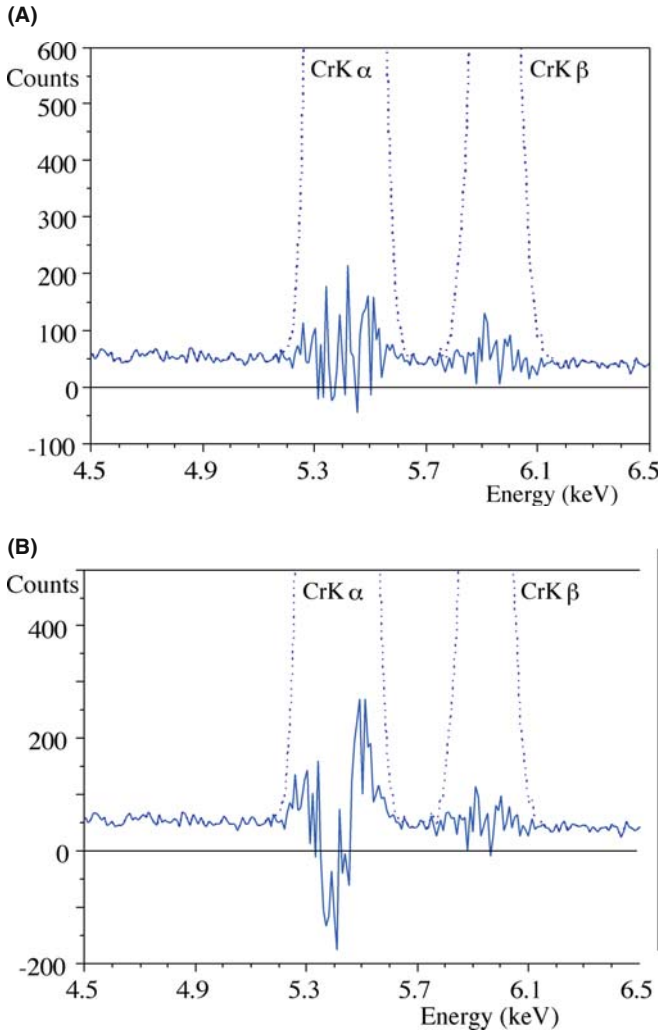

FIGURE 35.6. (A) A filtered Cr K-line family spectrum showing the residual background counts after the peaks have been removed for integration. The approximately linear residual intensity distribution indicates that the peaks matched well with the library standard stored in the computer. (B) A similar filtered spectrum showing the distorted residual spectrum characteristic of a poor fit with the library standard.

χ^2 OR CHI-SQUARED

Don't fear the math or the statistics. You'll rarely ever need to repeat it but you should know what your software is doing.

Any of the above methods is valid for obtaining values of the peak counts. They should all result in the same answer when used to quantify an unknown spectrum, so long as you apply the same method consistently to both the standard and the unknown.

Statham has reviewed the limitations of extracting peak intensities from X-ray spectra, with particular emphasis on low-keV lines. While aimed primarily at the EPMA community, almost all the issues in this paper are relevant to thin-film quantification.

Having obtained the peak counts, the next step is to insert the values into the Cliff-Lorimer equation and know the correct value of the k-factor. So we now need to discuss the various ways to obtain k_{AB}.

35.4 DETERMINING *k*-FACTORS

Remember that the k-factor is **not** a constant. It is a sensitivity factor that will vary not only with the X-ray detector, the microscope, and the analysis conditions, but also with your choice of background subtraction and peak-integration methods. So values of k-factors can be sensibly compared *only* when they were obtained under identical conditions. We will return to this point at the end of this section when we look at various sets of k-factors published in the literature. There are two ways you can determine k-factors

- Experimental determination using standards.
- Calculation from first principles.

The first method is slow and laborious but gives the most accurate values. The second method is quick and painless but the results are less reliable. You might wonder—can k-factors even depend on the previous user of the TEM?

k-FACTOR VERSUS ζ FACTOR

There are no generally accepted standards that meet all the above criteria for ideal k-factor determination, which is a major limitation to this approach and is overcome by the pure-element standards used in the ζ-factor method, which we describe later.

35.4.A Experimental Determination of k_{AB}

If you have a thin specimen of known composition, C_A, C_B etc., then all you have to do, in principle, is place that specimen in the microscope, generate a spectrum, obtain values of I_A, I_B, etc., and insert those values in the Cliff-Lorimer equation 35.2. Since you know C_A and C_B the only unknown is k_{AB}. However, there are several precautions that you must take before this procedure can be used

- The standard must be a well-characterized specimen, and it is usually best if it is single phase.
- The standard must be capable of being thinned to electron transparency. Ideally, when the specimen is thin there should be no significant absorption or fluorescence of the X-rays from the elements A, B, etc., that you wish to analyze.
- You must be sure that the thinning process did not induce any chemical changes (this is discussed in some detail in Chapter 10).
- It must be possible to select thin regions that are characteristic of the chemistry of the bulk specimen.
- You must be sure that the thin foil is stable under the electron beam at the voltage you intend to use for analysis.

This last point may often be the limiting factor in your choice of standards because, as we saw in Section 4.6, you have to take care to avoid not only direct knock-on damage, but also sputtering effects, which occur at voltages substantially below the threshold for direct atom displacement. Obviously, both these problems become greater as the beam voltage increases.

The National Institute of Standards and Technology (NIST) has issued a thin standard containing the elements Mg, Si, Ca, and Fe and O (SRM #2063 and subsequently #2063A). Unfortunately, X-rays from the lighter elements in this standard film are absorbed significantly in the film, and also in the detector and so a correction to the measured k-factor is necessary and NIST has not re-issued the standard.

It is best to use your own judgment in choosing standards, and also make use of the knowledge gained in previous k-factor studies.

Cliff and Lorimer's approach using mineral standards had three advantages.

- Crushing is an easy way to make thin flakes and does not affect the chemistry.
- The mineral stoichiometry is usually well known.
- The minerals chosen all contained Si, thus permitting the creation of a whole series of k_{ASi} factors.

The drawbacks are that the mineral specimens often contain more than one phase, or may be naturally non-stoichiometric. Clearly, some prior knowledge of the mineralogy of the specimen is essential in order to be able to select the right spectrum to use as a standard. Also Si K_α X-rays at ~1.74 keV are liable to be absorbed in the XEDS detector, so there may be a systematic difference in k-factors determined with different detectors. Finally, silicate minerals often exhibit radiolysis i.e., chemical changes due to beam-induced breaking of bonds.

GLASS STANDARDS

Can be made completely homogeneous. Reproducible (one batch). No channeling complications.

Several alternative approaches have been proposed that attempt to avoid the problems with k_{ASi}

- Wood et al. generated a series of k_{AFe} factors to overcome the Si absorption and the beam-sensitivity problems.
- Graham and Steeds used crystallized microdroplets which were routinely thin enough and retained their stoichiometry.
- Kelly used rapidly solidified droplets for the same reasons.
- Sheridan demonstrated the value of the NIST multi-element glasses.
- NIST created its own standard multi-element glass, as already noted.

Note also that there has been no new systematic determination of k-factors for many years, indicating the mature nature of the k-factor approach. But remember that you need factors for your TEM, your kV, etc.

DETERMINING *k*-FACTORS

A typical k-factor determination involves taking many spectra from different parts of the thin-foil standard. You must check both the homogeneity and the stability of the specimen. This is very time consuming, which is why so few analysts bother to do it properly.

In all cases, the bulk chemistry of the k-factor standard has to be determined by some technique with known accuracy, such as EPMA, atomic-absorption spectroscopy, or wet chemistry. Since all these techniques analyze relatively large volumes of material, it is best that the standard be single phase. However, because none of these techniques can determine if the specimen is homogeneous on a sub-micrometer scale, the only way to find out the level of homogeneity is to carry out many analyses within the AEM to confirm that any variation in your answer is within the expected X-ray statistical fluctuations.

Each spectrum should contain sufficient counts in the peaks of interest to ensure that the errors in the k-factor determination are at least less than $\pm 5\%$ relative and, if possible, less than $\pm 3\%$. So, now we need to consider the errors associated with the X-ray spectra.

35.4.B Errors in Quantification: The Statistics

An unfortunate aspect of the simple Cliff-Lorimer ratio equation is that it has relatively large errors associated with it. The very nature of the thin foil minimizes the problems of absorption and fluorescence, but also generates relatively few X-ray photons per incident electron, compared with bulk specimens. This effect is compounded by the small collection angle of the XEDS detector and the end result is that poor counting statistics are the primary source of error in most AEM quantifications. The best way you can limit these errors is to use higher-brightness sources, large electron probes, and thicker specimens (unless absorption is a problem, or spatial resolution is paramount) and, of course, C_s-correction of the probe helps. In any case you should be prepared to count for a long time, assuming that specimen drift and/or contamination don't compromise your data.

The rest of this section is pure statistics. If you know it, then jump ahead.

GAUSSIAN STATISTICS

Experimental results show that the X-ray counts in the spectrum obey Gaussian statistics. Hence, we can apply simple statistics to deduce the accuracy of any quantification.

Given that our characteristic peak is Gaussian, then the standard deviation σ is obtained from

$$\sigma = N^{\frac{1}{2}} \tag{35.8}$$

where N is the number of counts in the peak above the background. For a single measurement, there is a 67% chance that the measured value of N will be within 1σ of the true value of N. This chance increases to 95% for 2σ and 99.7% for 3σ. If we use the most stringent condition, then the relative error in any single measurement is

$$\text{Relative Error} = \frac{3N^{\frac{1}{2}}}{N}100\% \tag{35.9}$$

Clearly, the error decreases as N increases and hence, the emphasis throughout this chapter on the need to maximize the X-ray counts gathered in your spectra. Since the Cliff-Lorimer equation uses an intensity ratio, we can get a quick estimate of the error by summing the errors in I_A, I_B, and k_{AB} to give the total error in the composition ratio C_A/C_B.

Summing the errors in fact gives an overestimate of the error. Strictly speaking, we should add the standard deviations of the various terms in the Cliff-Lorimer equation in quadrature to give the standard deviation in the composition-ratio measurement σ_C using the expression

$$\left(\frac{\sigma_C}{C_A/C_B}\right)^2 = \left(\frac{\sigma_{k_{AB}}}{k_{AB}}\right)^2 + \left(\frac{\sigma_{I_A}}{I_A}\right)^2 + \left(\frac{\sigma_{I_B}}{I_B}\right)^2 \tag{35.10}$$

So we can determine the error for each datum point in this manner. If we are determining the composition of a single-phase region (for example, when determining a k-factor) then we can reduce the error by combining

the results from n different measurements of the intensity ratio I_A/I_B. The total absolute error in I_A/I_B at a given confidence limit is obtained using the student's t distribution. For example, in this approach the error is given by

$$\text{Absolute Error} = \frac{(t_{95})^{n-1} S}{n^{\frac{1}{2}}} \qquad (35.11)$$

where $t_{95}{}^{n-1}$ is the student's t value at the 95% confidence limit for n measurements of k_{AB}. You can find lists of student's t values in any statistics text (see, e.g., Larsen and Marx) or on the Web (e.g., URL #1). Obviously, you could choose a lower or higher confidence level. S is the standard deviation for n measurements where

$$S = \left(\sum_{n=1}^{n} \frac{(N_i - N)^2}{n-1} \right)^{1/2} \qquad (35.12)$$

So by increasing the number of measurements n, you can reduce the absolute error in k_{AB}. With enough measurements and a good homogeneous specimen, you can reduce the errors in the value of k_{AB} to $\pm 1\%$, as we will see in the example below. However, remember that this figure must be added to the errors in I_A and I_B. From equation 35.8 it is easy to determine that if we accumulate 10,000 counts in the peak for element A then the error at the 99% confidence limit is $[3\ (10{,}000)^{1/2}/10{,}000] \times 100\%$, which is $\sim 3\%$. Using equation 35.10 and a similar value for I_B you get a total error in C_A/C_B of $\sim \pm 4.5\%$. Now you see again why 'counts, counts, and more counts' is the mantra for thin-foil analysts.

If you take the time to accumulate 100,000 counts for I_A and I_B the total error is reduced to $\sim \pm 1.7\%$, which represents about the best accuracy that can be expected for quantitative XEDS analysis in the AEM. This is an accuracy that almost no one ever takes the time to achieve.

It is appropriate here to go through an illustration of a k_{AB} determination using experimental data. Before deciding that a particular specimen is suitable, it should be checked for its level of homogeneity: there is a well-established criterion for this. If we take the average value N of many composition determinations, and all the data points fall within $\pm 3(N)^{1/2}$ of N then the specimen is homogeneous. In other words, this is our definition of 'homogeneous.' There are more rigorous definitions but the general level of accuracy in thin-foil analysis is such that there is no need to be so stringent.

An example: A homogenized thin foil of Cu-Mn solid solution was used to determine k_{CuMn}. The specimen was first analyzed by EPMA and found to be 96.64 wt% Cu and 3.36 wt% Mn. Since our accuracy is increased by collecting many spectra, a total of 30 were accumulated ($n = 30$ in equation 35.12). In a typical spectrum the Cu K_α peak contained 271,500 counts above background and the Mn K_α peak contained 10,800 counts. So if we insert these data into the Cliff-Lorimer equation we get

$$\frac{96.67}{3.36} = k_{CuMn} \frac{271{,}500}{10{,}800}$$

$$k_{CuMn} = 1.14.$$

To determine an error on this value of the k-factor, equation 35.11 must be used. The student's t analysis of the k-factors from the other 29 (yes 29!) spectra gives an error of $\pm$ 0.01 for a 95% confidence limit. This error of about $\pm 1\%$ relative is about the best that can be achieved using the experimental approach to k-factor determination, but remember that 30 individual spectra had to be accumulated from different regions of a well-characterized thin foil.

STUDENT'S *t* DISTRIBUTION

More statistics but with much more interesting origins.

So it takes a real effort to get quantitative data with errors $< \pm$ 5–10% relative. Bear this in mind when you read any paper in which compositions are given to better than a rounded $\pm$ 5% (such as the EPMA data in our own example).

THIN-FOIL COMPOSITIONS

Any thin-foil composition data given with decimal points must be really scrutinized to see if they were obtained via a procedure such as that outlined here.

Otherwise they are just plain wrong.

Tables 35.1 and 35.2 summarize many of the available k-factor data in the published literature. You should go and read the original papers, particularly if you want to find out what standards and what conditions were used in their determination.

35.4.C Calculating k_{AB}

While it is clear that many of the values in these k-factor tables are very similar, the differences cannot be

TABLE 35.1 Experimentally Determined k_{ASi} and k_{AFe} Factors for K_α X-rays

Element (A)	k_{ASi} (1) 100 kV	k_{ASi} (2) 100 kV	k_{ASi} (3) 120 kV	k_{ASi} (4) 80 kV	k_{ASi} (5) 100 kV	k_{ASi} (5) 200 kV	k_{AFe} (6) 120 kV	k_{ASi} (7) 200 kV
Na	5.77	3.2	3.57 ± 0.21	2.8 ± 0.1	2.17	2.42		3.97 ± 2.32
Mg	2.07 ± 0.1	1.6	1.49 ± 0.007	1.7 ± 0.1	1.44	1.43	1.02 ± 0.03	1.81 ± 0.18
Al	1.42 ± 0.1	1.2	1.12 ± 0.03	1.15 ± 0.05			0.86 ± 0.04	1.25 ± 0.16
Si	1.0	1.0	1.0	1.0	1.0	1.0	0.76 ± 0.004	1.00
P			0.99 ± 0.016				0.77 ± 0.005	1.04 ± 0.12
S			1.08 ± 0.05		1.008	0.989	0.83 ± 0.03	1.06 ± 0.12
Cl					0.994	0.964		1.06 ± 0.30
K		1.03	1.12 ± 0.27	1.14 ± 0.1			0.86 ± 0.014	1.21 ± 0.20
Ca	1.0 ± 0.07	1.06	1.15 ± 0.02	1.13 ± 0.07			0.88 ± 0.005	1.05 ± 0.10
Ti	1.08 ± 0.07	1.12	1.12 ± 0.046				0.86 ± 0.02	1.14 ± 0.08
V	1.13 ± 0.07			1.3 ± 0.15				1.16 ± 0.16
Cr	1.17 ± 0.07	1.18	1.46 ± 0.03				0.90 ± 0.006	
Mn	1.22 ± 0.07	1.24	1.34 ± 0.04				1.04 ± 0.025	1.24 ± 0.18
Fe	1.27 ± 0.07	1.30	1.30 ± 0.03	1.48 ± 0.1			1.0	1.35 ± 0.16
Co							0.98 ± 0.06	1.41 ± 0.20
Ni	1.47 ± 0.07	1.48	1.67 ± 0.06				1.07 ± 0.006	
Cu	1.58 ± 0.07	1.60	1.59 ± 0.05		1.72	1.50	1.17 ± 0.03	1.51 ± 0.40
Zn	1.68 ± 0.07				1.74	1.55	1.19 ± 0.04	1.63 ± 0.28
Ge	1.92							1.91 ± 0.54
Zr								3.62 ± 0.56
Nb							2.14 ± 0.06	
Mo	4.3		4.95 ± 0.17				3.8 ± 0.09	
Ag	8.49		12.4 ± 0.63				9.52 ± 0.07	6.26 ± 1.50
Cd	10.6				9.47	6.2		
In								7.99 ± 1.80
Sn	10.6							8.98 ± 1.48
Ba					29.3	17.6		21.6 ± 2.6

TABLE 35.2 Experimentally Determined k_{ASi} and k_{AFe} Factors for L X-rays

Element (A)	k_{ASi} (8) 100 kV	k_{ASi} (5) 100 kV	k_{ASi} (5) 200 kV	k_{ASi} (9) 100 kV	k_{AFe} (6) 120 kV	k_{ASi} (7) 200 kV
Cu		8.76	12.2			
Zn		6.53	6.5			8.09 ± 0.80
Ge						4.22 ± 1.48
As						3.60 ± 0.72
Se						3.47 ± 1.11
Sr					1.21 ± 0.06	
Zr					1.35 ± 0.1	2.85 ± 0.40
Nb					0.9 ± 0.06	
Mo				2.0		
Ag	2.32 ± 0.2				1.18 ± 0.06	2.80 ± 1.19
In					2.21 ± 0.07	2.86 ± 0.71
Cd		2.92	2.75			
Sn	3.07 ± 0.2					
Ba		3.38	2.94			3.36 ± 0.58
Ce				1.4		
Sn	3.1 ± 0.2			1.3		
W	3.11 ± 0.2			1.8		3.97 ± 1.12
Au	4.19 ± 0.2	4.64	3.93		3.1 ± 0.09	4.93 ± 2.03
Pb	5.3 ± 0.2	4.85	4.24	2.8		5.14 ± 0.89

All L-line *k*-factors use the total L counts from the L_α and L_β lines.
Sources: (1) Cliff and Lorimer (1975), (2) Wood et al. (1981), (3) Lorimer et al. (1977), (4) McGill and Hubbard (1981), (5) Schreiber and Wims (1981), (6) Wood et al. (1984), (7) Sheridan (1989), (8) Goldstein et al. (1977), (9) Sprys and Short (1976).

accounted for by X-ray statistics alone. Some of the differences arise due to the choice of standard and the reproducibility of the standard. Other differences arise because the data were obtained under different conditions, such as different peak-integration routines. Therefore, the point made at the beginning of this section is worth repeating: the *k*-factors are not standards; they are sensitivity factors.

The only conditions under which you can expect the *k*-factors obtained on different AEMs to be identical are if you use the *same* standard at the *same* accelerating voltage, *same* detector configuration, *same* peak integration, and *same* background-subtraction routines. Even then there will be differences if one or more of the measured X-ray lines are not gathered by the detector with 100% efficiency; the X-ray may be either absorbed by the detector or it may be too energetic and pass straight through the detector.

You may not be able to obtain a suitable standard. For example, you might be working in a system in which no stoichiometric phases exist. You might not need a standard because accuracy might not be critical but you still need a quick analysis. Under such circumstances you can calculate an approximate *k*-factor. The programs necessary to calculate k_{AB} are stored in the XEDS computer and will give you a value of k in a fraction of a second. The calculated value should be accurate to within ±20% relative. This level of accuracy might be all you need to draw a sensible conclusion about the material you are examining (in which case, you can almost rely on a simple peak-height measurement). In general, if you can avoid the tedious experimental approach, then do so.

QUICK

Calculating *k*-factors is the recommended approach when a quick answer is required and the highest accuracy is not essential.

The expression for calculating the *k*-factor from first principles is derived in the paper by Williams and Goldstein. The derivation gives a good illustration of the relationship between bulk and thin-film analysis, and provides insight into the details of X-ray interactions with solids. However, at this stage you don't need to know the details of this derivation so we'll simply state the final expression

$$k_{AB} = \frac{1}{Z} = \frac{(Q\omega a)_B A_A}{(Q\omega a)_A A_B} \qquad (35.13)$$

The subscripts A, B denote the elements A, B of atomic weight A_A and A_B. This expression derives from the physics of X-ray generation. An electron passing close to an atom in the specimen has first to ionize that atom and this is governed by Q_A, the ionization cross section (sometimes given by σ; go back and check equation 4.1). An ionized atom does not necessarily give off a characteristic X-ray when it returns to ground state and the fraction of ionizations that do generate an X-ray is governed by the fluorescence yield for the characteristic X-rays, ω_A (go back and check equation 4.6) The remaining term '*a*' is the relative-transition probability. This term takes account of the fact that if a K-shell electron is ionized and returns to ground state through X-ray emission, it can emit either a K_α or K_β X-ray. You may remember that we listed the relative weights of the various K, L, and M families of X-ray lines in Table 4.1.

THE *k*-FACTOR CALCULATION

Elements A and B; atomic weight A_A and A_B
Ionization cross sections Q_A and Q_B
Fluorescence yield ω_A and ω_B
Relative transition probability, a
Detector efficiency, ε_A and ε_B

As we mentioned at the start of the discussion on quantification, the Cliff-Lorimer *k*-factor for thin-foil analysis is related to the atomic-number correction factor (Z) for bulk specimen analysis. From equation 35.13, we can easily see what experimental factors determine the value of k

- The accelerating voltage is a variable since Q is strongly affected by the kV.
- The atomic number affects ω, A, and a.
- The choice of peak-integration method will also affect a.

Therefore, in order to calculate and compare different *k*-factors, it is imperative to define these conditions very clearly, as we have taken pains to emphasize.

Equation 35.13 assumes that equal fractions of the X-rays generated by elements A and B are collected and processed by the detector. This assumption will only be true if the same detector is used and the X-rays are neither strongly absorbed by, nor pass completely through, the detector. However, as we have already seen in Chapter 32, X-rays below ~1.5 keV are absorbed significantly by Be window and X-rays above ~20 keV pass through a 3 mm Si detector with ease. Under these circumstances, it is necessary to modify the *k*-factor expression, equation 35.13, in the following manner

$$k_{AB} = \frac{1}{Z} = \frac{(Q\omega a)_A}{(Q\omega a)_B}\frac{A_B}{A_A}\frac{\varepsilon_A}{\varepsilon_B} \qquad (35.14)$$

The symbol ε represents simply a detector efficiency term plotted back in Figure 32.7 that we can write as follows.

$$\varepsilon_A = \exp\left(-\left[\frac{\mu}{\rho}\right]_{Be}^{A}\rho_{Be}t_{Be}\right)\exp\left(-\left[\frac{\mu}{\rho}\right]_{Au}^{A}\rho_{Au}t_{Au}\right)$$
$$\exp\left(-\left[\frac{\mu}{\rho}\right]_{Si}^{A}\rho_{Si}t_{Si}\right)\left\{1-\exp\left(-\left[\frac{\mu}{\rho}\right]_{Si}^{A}\rho_{Si}t'_{Si}\right)\right\} \quad (35.15)$$

The first term accounts for absorption (via the mass absorption coefficients, μ/ρ) of X-rays from element A passing through the Be window. It should of course be modified for different windows and it disappears for windowless detectors. The second term covers absorption in the Au contact layer and the third term accounts for the Si dead layer. These two terms will have different values for different contact elements, IG dead layers, and SDDs which have very thin dead layers and side contact layers. The last term adjusts the *k*-factor for X-rays that *do not* deposit their energy in the active region of a detector which has density ρ and thickness t'. Typical values of t' (~ 3 mm for Si(Li) and IG but ~ 1 mm for SDDs) were discussed in Chapter 32. An IG detector will more efficiently stop high-energy X-rays, since it is designed to detect them preferentially, while an SDD will be less efficient since it is generally much thinner than a Si(Li) or IG. In fact, much of the effort over the last 20 years to improve detector technology that we discussed in detail in Chapter 32, minimizes the effects of equation 35.15 on the *k*-factor.

While equations 35.14 and 35.15 are simple for a computer to solve, the values that have to be inserted in the equations for the various terms are not always well known, or cannot be measured accurately. For example, we do not know the best value of Q for many elements in the range of voltages typically used in the AEM (100–400 kV). There are considerable differences of opinion in the literature concerning the best way to choose a value for Q. The two major approaches used are

- Assume various empirical parameterization processes (e.g., Powell).
- Interpolate values of Q to give the best fit to experimental *k*-factors (Williams et al.).

The other major variable in equation 35.15 is the Be-window thickness which is nominally 7.5 μm but in practice may be 3–4× thicker. Tables 35.3A and 35.3B list calculated *k*-factors obtained using various expressions for Q. As you can see, the value of k may easily vary by $>\pm 10\%$, particularly for the lighter and the heavier elements. This variation is due to the uncertainties in the detector-efficiency terms in equation 35.14. The values of k_{AB} for the L lines are even less accurate than for the K lines mainly because the values of Q for the L lines are somewhat speculative. There are no data available for calculated *k*-factors for M lines. Under these circumstances, experimental determination is the only approach (or choose different materials to study). This point again emphasizes the advantages of K-line analysis where possible. If you are unfortunate enough to have heavy elements (say $Z > 60$) in your specimen, the L or M lines, which may be the strongest in a spectrum from a Si(Li) detector, will undoubtedly give rise to greater errors than the K lines, which may only be detectable with an IG system.

TABLE 35.3A Calculated k_{AFe} Factors for K_α X-rays Using Different Theoretical Cross Sections

Element A	k_{MM}^*	k_{GC}^*	k_P^*	k_{BP}^*	k_{SW}^*	k_Z^*
Na	1.42	1.34	1.26	1.45	1.17	1.09
Mg	1.043	0.954	0.898	1.03	0.836	0.793
Al	0.893	0.882	0.777	0.877	0.723	0.696
Si	0.781	0.723	0.687	0.769	0.638	0.623
P	0.813	0.759	0.723	0.803	0.671	0.663
S	0.827	0.776	0.743	0.817	0.688	0.689
K	0.814	0.779	0.755	0.807	0.701	0.722
Ca	0.804	0.774	0.753	0.788	0.702	0.727
Ti	0.892	0.869	0.853	0.888	0.807	0.835
Cr	0.938	0.925	0.917	0.936	0.887	0.909
Mn	0.98	0.974	0.970	0.979	0.953	0.965
Fe	1.0	1.0	1.0	1.0	1.0	1.0
Co	1.063	1.069	1.074	1.066	1.096	1.079
Ni	1.071	1.085	1.096	1.074	1.143	1.23
Cu	1.185	1.209	1.227	1.19	1.31	1.24
Zn	1.245	1.278	1.305	1.255	1.44	1.32
Mo	3.13	3.52	3.88	3.27	3.84	3.97
Ag	4.58	5.41	6.23	4.91	5.93	6.28

TABLE 35.3B Calculated k_{AFe} Factors for L X-rays Using Different Theoretical Cross Sections

Element	k_{MM}^*	k_P^*	k_{BP}^*	k_{SW}^*	k_Z^*
Sr*	1.73	1.33	1.32	1.64	1.39
Zr*	1.62	1.26	1.24	1.51	1.33
Nb*	1.54	1.21	1.18	1.43	1.28
Ag*	1.43	1.16	1.09	1.26	1.26
Sn	2.55	2.09	1.93	2.21	2.30
Ba	2.97	2.52	2.25	2.49	2.83
W	3.59	3.37	2.68	2.80	3.88
Au	3.94	3.84	2.94	3.05	4.43
Pb	4.34	4.31	3.05	3.34	4.97

All L-line *k*-factors use the total L counts from the L_α and L_β lines.
Cross sections used in the calculations are: MM (Mott-Massey); GC (Green-Cosslett); P (Powell); BP (Brown-Powell); SW (Schreiber-Wims); Z (Zaluzec).

AFTER A SERVICE

If your detector is replaced or serviced, which is not an unusual occurrence on an AEM, then the new detector parameters must be inserted into the software.

The combination of uncertainties in Q and in the detector parameters is the reason why calculated k-factors are not very accurate, usually no better than ±10–20% relative. The computer system attached to the AEM should have predetermined values of all the terms in equations 35.14 and 35.15 stored in its memory. You don't usually have control over which particular parameters are being used. However, you should at least find out from your technical support the sources of the values of Q, ω, and a in your computer. You should then carry out a cross-check calculation with a known specimen to ensure that the calculated k-factor gives a reasonable answer.

BLACK BOXES

All software packages use preset values in their calculations and these may vary from package to package.

We cannot recommend a best set of values for Q, ω, and a, but the values of Q given by Powell, ω from Bambynek et al., and a from Schreiber and Wims have often been used. Also we can't give you specific detector parameters, so you should read the literature from your XEDS manufacturer. The values of μ/ρ that are still widely accepted are those determined by Heinrich although there is still considerable uncertainty in μ/ρ values for low-energy X-rays from the lighter elements. If you use the DTSA program from NIST (see Section 1.6), you may find that it predicts a worse value.

Figure 35.7A and B shows a comparison of the two methods of k-factor determination. The experimental data are shown as individual points with error bars and the solid lines represent the range of calculated k-factors, depending on the particular value of Q used in equation 35.14. The relatively large errors possible in the calculated k-factors are clearly seen and comparison of the K-line data in Figure 35.7A with the L-line data in Figure 35.7B again emphasizes the advantages of using K lines for the analysis where possible. Similar data for M lines are almost non-existent.

We can summarize the k-factor approach to analysis in the following way

- The Cliff-Lorimer equation has the virtue of simplicity; all you have to do is specify all the variables and treat the standard and unknown in an identical manner.
- You are better off calculating k_{AB} if you prefer speed to accuracy; experimental determination is best if you wish to have a known level of confidence in the numbers that you produce.

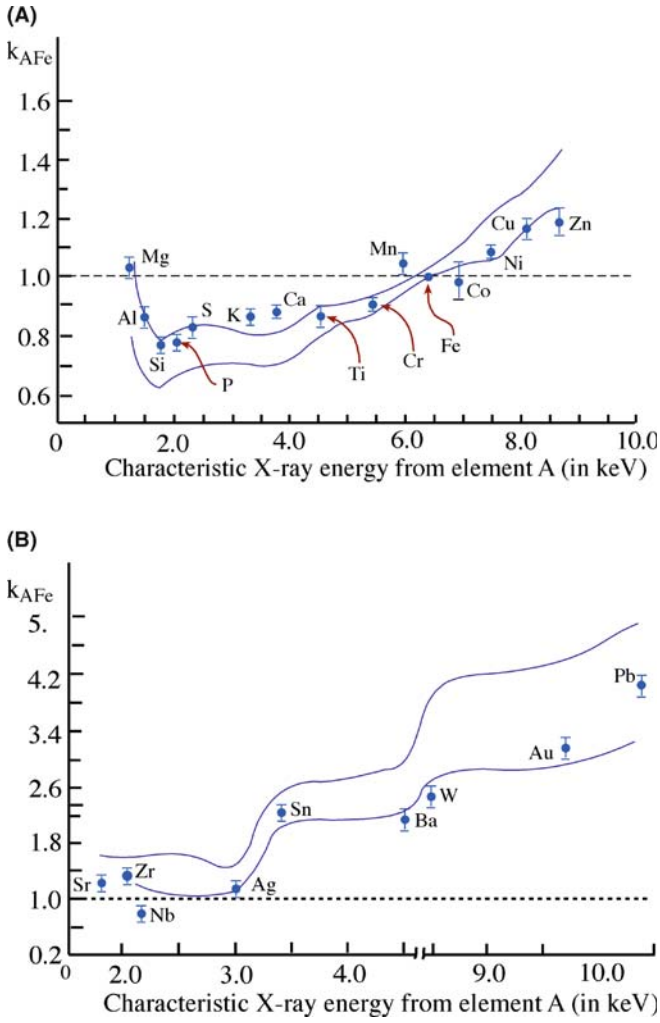

FIGURE 35.7. (A) Experimental k_{AFe} factors as a function of X-ray energy for the K_α X-rays from a range of elements A with respect to Fe. The solid lines represent the spread of calculated k-factors using different values for the ionization cross section. (B) Similar data to (A) for L_α lines from relatively high-Z elements. The errors in the calculated values of k are large, reflecting the uncertainties in L-line ionization cross sections.

35.5 THE ZETA-FACTOR METHOD

The Cliff-Lorimer ratio method is > 30 years old and, while it is simple in concept, the need for a k-factor combined with the difficulties of finding the right standard specimen, and calculating an accurate enough k-factor to solve a specific problem are significant limiting factors. These can be overcome if, instead of using a ratio method, we go back to the fundamentals of X-ray analysis as originally developed for the EPMA (based on equation 35.1) wherein pure-element standards are used. Pure-element standards have the distinct advantages of being easy to fabricate and they don't change composition during thinning or under beam damage. This approach, developed by Watanabe and Horita in Japan, is termed the zeta (ζ) factor method. A review of the development of the method and the pros and cons of

ζ-factors versus *k*-factors was given by Watanabe and Williams in 2006.

The major experimental drawback to ζ-factors is that the method requires in-situ measurement of the probe current hitting your specimen. Unfortunately, despite the fact that beam-current measurement is standard on almost all SEMs and every EPMA, commercial AEMs don't come equipped with this capability, emphasizing the point made some while ago in Chapter 33 that AEMs are really modified TEMs and XEDS analysis is still a bit of an afterthought.

But, if you can measure the current in situ, e.g., with a specimen holder within which a Faraday cup is embedded, life gets much easier. In a thin-foil specimen, we can assume that the characteristic X-ray intensity is proportional to the mass thickness, ρt, if X-ray absorption and fluorescence are negligible. Therefore, we can define the ζ-factor for pure element A as

$$\rho t = \zeta_A \frac{I_A}{C_A} \tag{35.16}$$

Where

$$\zeta \equiv \frac{A}{CN_0 Q\omega a i} \tag{35.17}$$

where the only new terms are the beam current i, and Avogadro's number N_0. Under these conditions, the ζ-factor is dependent on the X-ray energy, the kV, and the beam current. The first two are constant for any experiment and the third you have to measure. The ζ-factor is independent of specimen thickness, composition, and density which, as we shall see later, makes any absorption correction trivial.

So we can write similar equations for all the other pure elements in our specimen

$$\rho t = \zeta_B \frac{I_B}{C_B} \tag{35.18}$$

When we know the ζ-factors for A and B, C_A, C_B, and ρt can be expressed from equations 35.16 and 35.18, assuming $C_A + C_B = 1$ in a binary system:

$$C_A = \frac{I_A \zeta_A}{I_A \zeta_A + I_B \zeta_B},$$
$$C_B = \frac{I_B \zeta_B}{I_A \zeta_A + I_B \zeta_B} \quad \rho t = I_A \zeta_A + I_B \zeta_B \tag{35.19}$$

Therefore, we can determine C_A, C_B, and ρt simultaneously just by measuring X-ray intensities. It is simple to rearrange equation 35.19 to compare with the Cliff-Lorimer ratio equation (equation 35.2) and equation 35.20 is just as simple to apply, but *k*-factors are no longer required, just ζ-factors.

$$\frac{C_A}{C_B} = \frac{I_A \zeta_A}{I_B \zeta_B} \tag{35.20}$$

As we'll see below, absorption and fluorescence-correction terms can be combined directly with equation 35.19. To determine the ζ-factors, you just measure X-ray characteristic intensities (above the background)

TABLE 35.4 ζ-Factor Values Estimated from Experimental X-ray Spectra from the NIST SRM2063a Glass Thin Film in a 200-keV FEG-STEM JEM-2010F with an ATW Detector and in a 300-keV FEG-DSTEM VG HB603 with a Windowless Detector.

	ζ-factor (kg electron/m/photon)			ζ-factor (kg electron/m/photon)	
Element (Z)	200 keV ATW	300 keV Windowless	Element (Z)	200 keV ATW	300 keV Windowless
N	16,505.2±1,537	720.2±58.0	Mn	1,752.2±41.8	706.0±17.3
O	4,092.3±205.5	583.5±31.3	Fe	1,790.5±42.7	721.1±17.7
F	20,548.2±4,852.8	891.6±214.5	Co	1,919.0±45.8	772.0±18.9
Ne	5,345.6±702.1	635.8±85.5	Ni	1,950.0±46.5	783.2±19.2
Na	2,819.6±221.9	571.7±46.3	Cu	2,163.4±51.6	867.3±21.2
Mg	1,847.9±95.0	501.4±26.6	Zn	2,300.1±54.9	920.1±22.5
Al	1,510.2±56.2	483.6±18.6	Ga	2,541.8±60.7	1,014.4±24.8
Si	1,369.5±41.3	467.5±14.6	Ge	2,762.1±65.9	1,099.5±26.9
P	1,691.2±50.4	484.3±13.4	As	3,009.5±71.8	1,194.7±29.2
S	1,488.6±40.0	507.6±14.2	Se	3,328.6±79.4	1,317.7±32.2
Cl	1,465.5±37.3	528.0±13.9	Br	3,531.1±84.3	1,397.7±34.2
Ar	1,532.7±37.8	579.3±14.9	Kr	3,890.2±92.8	1,534.6±37.6
K	1,405.5±34.2	545.7±13.8	Rb	4,182.3±99.8	1,644.2±40.2
Ca	1,377.6±33.2	544.3±13.6	Sr	4,476.8±106.8	1,755.7±43.0
Sc	1,522.5±36.5	607.0±15.0	Y	4,786.6±114.2	1,871.6±45.8
Ti	1,553.4±37.2	622.8±15.4	Zr	5,185.4±123.7	2,019.8±49.4
V	1,632.3±39.0	656.5±16.1	Nb	5,578.9±133.1	2,164.8±53.0
Cr	1,654.6±39.5	666.5±16.4	Mo	6,088.3±145.3	2,353.4±57.6

from pure-element thin films with known composition and thickness, rather than trying to find a suitable set of standards, such as those listed in the references for Tables 35.1 and 35.2. Pure-element standards are more routinely available than the various multi-element, thin-film standards that have been used for *k*-factor determination over the last 30 years or so. You can determine an entire set of the ζ-factors for K-shell X-ray lines from a single spectrum from the National Institute of Standards and Technology (NIST) thin-film glass standard reference material (SRM) 2063. Table 35.4 lists such a set of ζ-factors obtained from the NIST standard SRM 2063a, which is a thinner version of SRM 2063. Its composition is known to a high degree of accuracy, as is its thickness and density but, unfortunately, it is now out of production.

There's much more about the ζ-factor in the companion text. Despite its obvious advantages, the ζ-factor approach is not yet commercially available; however, it can be downloaded from the book Web site (URL #2).

35.6 ABSORPTION CORRECTION

The point at which the simple Cliff-Lorimer approach breaks down is when the thin-foil criterion is invalid. Then the X-ray counts from your specimen are not a function of Z alone and absorption and (very occasionally) fluorescence invalidate the simple criterion. The effects of absorption are much more of a problem than fluorescence, so let's look at absorption first.

Preferential absorption of the X-rays from one of the elements in your specimen means that the detected X-ray counts will be less than the generated counts and so C_A is no longer simply proportional to I_A. So you have to modify the *k*-factor to take into account the reduction in I_A. This problem can arise (a) if your specimen is too thick, (b) if one or more of the characteristic X-rays has an energy less than ~1–2 keV (i.e., light-element analysis) or (c) when you have X-ray lines in your spectrum that differ in energy by > 5–10 keV (because the lower energy X-ray is much more likely to be absorbed than the higher energy one).

If we define k_{AB} as the true sensitivity factor when the specimen thickness $t = 0$, then the effective sensitivity factor for a specimen in which absorption occurs is given by k_{AB}* where

$$k^*_{AB} = k_{AB}(\mathrm{ACF}) \tag{35.21}$$

So we can write

$$\frac{C_A}{C_B} = k_{AB}(\mathrm{ACF})\frac{I_A}{I_B} \tag{35.22}$$

The absorption-correction factor (ACF) is the A term in equation 35.13 and we can write it as

$$\mathrm{ACF} = \frac{\int_0^t \left\{ \varphi_B(\rho t)\; e^{-\left(\frac{\mu}{\rho}\right]^B_{\mathrm{Spec}} \rho t \,\mathrm{cosec}\,\alpha} \right\} d(\rho t)}{\int_0^t \left\{ \varphi_A(\rho t)\; e^{-\left(\frac{\mu}{\rho}\right]^A_{\mathrm{Spec}} \rho t \,\mathrm{cosec}\,\alpha} \right\} d(\rho t)} \tag{35.23}$$

In this expression $\varphi(\rho t)$ is the depth distribution of X-ray production (which is the ratio of the X-ray emission from a layer of element A/B (of thickness $\Delta\rho t$ at depth t in the specimen with density ρ) to the X-ray emission from an identical, but isolated film). The term $\left(\frac{\mu}{\rho}\right]^A_{\mathrm{Spec}}$ is the mass-absorption coefficient of X-rays from element A in the specimen and α is the detector take-off angle. Since the values of μ/ρ are often from old publications, the units are usually given in cm^2/gm rather than kg/m^2, so you may have to use ρ in gm/cm^3 and t in cm, rather than SI units (kg/m^3 and m, respectively). Obviously, the value of the ACF is unity when no absorption occurs. Typically, if the ACF is >10% we define the absorption as significant, since 10% accuracy is routinely attainable in quantitative analysis using experimental *k*-factors. Let's now look at each of the terms and the problems associated with determining their value.

Again, we recommend that you use the values of μ/ρ given by Heinrich. The value of μ/ρ for a particular X-ray (e.g., from element A) within the specimen is the sum of the mass-absorption coefficients for each element times the weight fraction of that element, so

$$\left(\frac{\mu}{\rho}\right]^A_{\mathrm{spec}} = \sum_i \left(\frac{C_i\mu}{\rho}\right]^A_i \tag{35.24}$$

where C_i is the fractional concentration of element i in the specimen such that

$$\sum_i C_i = 1 \tag{35.25}$$

The absorption of X-rays from element A by all elements i in the specimen is summed. The summation includes self-absorption by element A. Elements that may not be of interest in the experiment or that might not be detectable may still cause absorption.

The NiO-MgO example of this phenomenon occurs when Mg is being quantified in homogeneous NiO-MgO. The Mg K_α X-rays will be absorbed by oxygen, even if the O K_α X-ray is not of interest or cannot be detected because a Be-window detector is being used. This effect is shown in Figure 35.8, which shows an increase in the intensity ratio (Ni K_α/Mg K_α) as a function of thickness due to the increased absorption of the

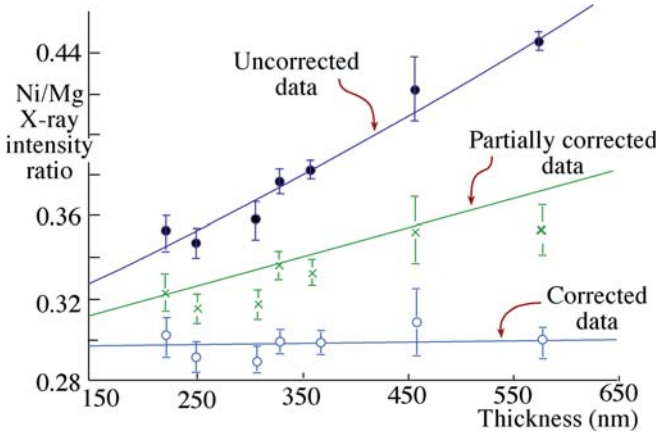

FIGURE 35.8. The upper curve shows the raw Ni K_α/Mg K_α intensity ratio as a function of thickness in a homogeneous specimen of NiO-MgO. The slope indicates strong absorption of Mg K_α X-rays. The middle curve shows the effect of correcting for absorption of the Mg K_α X-rays by Ni and the bottom line shows the effect of a further correction for absorption of the Mg K_α by O to give the expected horizontal line.

Mg K_α X-rays. (Absorption appears in an exponential term.) If we correct for the absorption by Ni, the slope of the line is reduced, but only when the effects of absorption by oxygen are taken into account does the slope become zero, as it should be for a homogeneous specimen.

In equation 35.22, we assume that the depth distribution of X-ray production $\varphi(\rho t)$ is a constant, and equal to unity. That is, a uniform distribution of X-rays is generated at all depths throughout the foil. This is a reasonable first approximation in thin foils, but in bulk specimens $\varphi(\rho t)$ is a strong function of t and so the measurement of $\varphi(\rho t)$ for bulk specimens is a well-established procedure. The few studies in thin specimens show an increase in $\varphi(\rho t)$ with specimen thickness, although the increase is no more than ~5% in foil thicknesses of < 300 nm. Therefore, the assumption appears reasonable since, if your specimen is thicker than 300 nm, you will have problems to worry about other than $\varphi(\rho t)$. The fact that we use a ratio of the two $\varphi(\rho t)$ terms in the absorption equation also helps to minimize the effects of this assumption.

We assume that $\varphi(\rho t)$ equals unity, then we can simply use equation 35.23 to give

$$\mathrm{ACF} = \left(\frac{\left[\frac{\mu}{\rho}\right]^{\mathrm{A}}_{\mathrm{Spec}}}{\left[\frac{\mu}{\rho}\right]^{\mathrm{B}}_{\mathrm{Spec}}}\right)\left(\frac{1 - e^{-\left(\left[\frac{\mu}{\rho}\right]^{\mathrm{B}}_{\mathrm{Spec}} \rho t \,\mathrm{cosec}\,\alpha\right)}}{1 - e^{-\left(\left[\frac{\mu}{\rho}\right]^{\mathrm{A}}_{\mathrm{Spec}} \rho t \,\mathrm{cosec}\,\alpha\right)}}\right) \qquad (35.26)$$

So we still need to know the values of ρ and t for our specimens.

The density of the specimen (ρ) can be estimated if you know the unit-cell dimensions, e.g., from CBED since

$$\rho = \frac{nA}{V\mathrm{N}} \qquad (35.27)$$

where n is the number of atoms of average atomic weight A in a unit cell of volume V, and N is Avogadro's number.

The absorption path length (t') is a major variable in the absorption correction. Fortunately, it is also the one over which you, the operator, have the most control. In the simplest case of a parallel-sided thin foil of thickness t at 0° tilt, the absorption path length, as shown in Figure 35.9, is given by

$$t' = t' \,\mathrm{cosec}\,\alpha \qquad (35.28)$$

where α is the detector take-off angle. To minimize this factor it is obvious that your specimen should be as thin as possible and the value of α as high as possible. There are many ways to determine the foil thickness, which we have discussed at various points in this text; they are summarized in Section 36.3. More recently, Banchet et al. (2003) have combined EELS measurements of relative specimen thickness with XEDS peak intensities to give a variation on the traditional, iterative absorption-correction process. No method is universally applicable, and few are either easy or accurate, so it's best to make thin specimens in the first place.

The value of α when your specimen is at the ideal 0° tilt is fixed by the design geometry of your AEM stage and the only way you can vary α is by tilting your specimen. As we have seen, there are good reasons not to tilt beyond about 10°, because of the increase in spurious X-rays, but if there is a severe absorption problem, then decreasing t' by tilting your specimen *toward* the detector is a sensible first step toward minimizing the problem. On some very old AEMs the detector may not be orthogonal to the axis of your specimen holder, in which case you've got a challenging exercise in solid geometry to determine α.

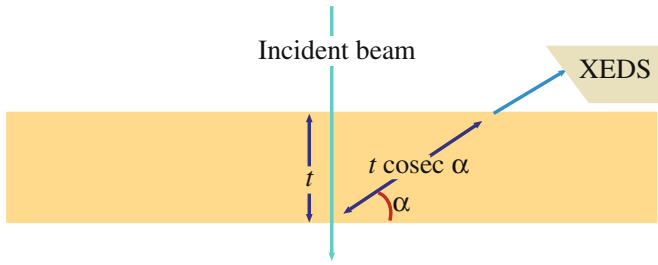

FIGURE 35.9. Relationship between the specimen thickness, t, and the absorption path length, t cosec α, for a take-off angle α.

HOW THICK?
Remember: it's rare that you'll know your specimen thickness as well as you would like.

So far we've assumed that our specimens are parallel sided, but this is uncommon. Many thin-foil preparation methods result in wedge-shaped foils, and under these circumstances the detector must always be looking toward the thin edge of the specimen so that the X-ray path length is minimized, as we already described in Figure 32.15. The only way to ascertain if this is a problem is to measure the thickness at each analysis point. Because this is such a tedious exercise, you should get round it by using the ζ-factor method, as we explain in the next section.

Because the specimen density ρ (and therefore the values of μ/ρ) varies with your specimen composition the complete absorption-correction procedure is an iterative process. The first step is to use the Cliff-Lorimer equation without any absorption correction and thus produce values for C_A and C_B. From these values, the computer performs a first-iteration calculation of μ/ρ and ρ, and generates modified values of C_A and C_B, and iterates again. Usually the calculation converges after two or three iterations.

In summary, there is substantial room for error in determining the various terms to insert into the ACF. For example, the ACF for k_{NiAl} in Ni_3Al, which is a strongly absorbing system, varies from ~5.5 to ~12% when the specimen doubles in thickness from 40 to 80 nm. This change is still quite small and within the limits of all but the most accurate analyses. In FeNi, which is a weakly absorbing system, a similar change in thickness would change the ACF for k_{FeNi} from ~0.6 to ~1.3%, which is negligible. So while we've spent a fair bit of time introducing you to the absorption correction, the final message is clear.

CLIFF-LORIMER ACCURACY?
The Cliff-Lorimer approach only incurs large errors in strongly absorbing systems and/or very thick specimens.

35.7 THE ZETA-FACTOR ABSORPTION CORRECTION

So, if significant absorption is unavoidable, information about your specimen density and thickness is required at each analysis position, in order to apply the absorption correction. Obviously, this is the major limitation, since independent measurements are required for the specimen density and thickness and inaccuracies in such measurements may cause further errors in quantification. In fact, the ζ-factor method was originally proposed in order to overcome these limitations and difficulties associated with the absorption correction because, if we substitute equation 35.16 into equation 35.22, the ρt term can be eliminated

$$\frac{C_A}{C_B} = k_{AB}\left(\frac{I_A}{I_B}\left[\frac{(\mu/\rho)^A_{sp}}{(\mu/\rho)^B_{sp}}\right]\left\{\frac{1-\exp\left[-(\mu/\rho)^B_{sp}\,\zeta_A(I_A/C_A)\,\mathrm{cosec}(\alpha)\right]}{1-\exp\left[-(\mu/\rho)^A_{sp}\,\zeta_A(I_A/C_A)\,\mathrm{cosec}(\alpha)\right]}\right\}\right) \tag{35.29}$$

If you've determined ζ-factors, then the k-factor can be substituted in the above equation since

$$k_{AB} = \frac{\zeta_A}{\zeta_B} \tag{35.30}$$

So the ζ-factor overcomes the two major limitations of the Cliff-Lorimer method by avoiding the tedium of preparing multiple thin-foil standards and making multiple thickness and density measurements at each analysis point when significant X-ray absorption is occurring. That's why we introduce its depth in the companion text and suggest strongly that the serious X-ray analyst use this approach.

35.8 THE FLUORESCENCE CORRECTION

X-ray absorption and fluorescence are intimately related because a primary cause of X-ray absorption is the fluorescence of another X-ray (such as the fluorescence of Si K_α X-rays in the XEDS detector which gives rise to the escape peak). You might think, therefore, that fluorescence corrections should be as widespread as absorption corrections. However, this is not the case for the following reasons. Strong absorption effects occur when there is a small amount of one element whose X-rays are being absorbed by the presence of a relatively large amount of another element. The absorption of Al K_α X-rays by Ni in Ni_3Al is a classic example. In this case, Ni X-rays are indeed fluoresced as a result of the absorption of Al K_α X-rays. However, there is a relatively small

increase in the total number of Ni X-rays because Ni is the dominant element; the relative decrease in the Al K_α intensity is large because Al is the minor constituent. In this particular example there is a further reason why fluorescence of Ni X-rays is ignored; it is the Ni L_α X-rays which are fluoresced by the absorption of Al K_α X-rays. The Ni L X-rays are not the ones that we use for analysis anyhow, since the higher energy Ni K X-rays are not absorbed or fluoresced.

In the rare case that fluorescence occurs to a degree that limits the accuracy of your analysis, read the detailed discussion given by Anderson et al. Practical examples of the fluorescence correction are hard to come by and a classic case is Cr in stainless steels where the minor Cr K_α line is fluoresced by the major Fe K_α line, giving rise to an apparent increase in Cr content as the foil gets thicker.

DON'T WORRY ABOUT FLUORESCENCE

Fluorescence is usually a minor effect and often occurs for X-rays that are not of interest. (So don't worry if you know you needn't!)

35.9 ALCHEMI

We told you early on in this chapter to acquire your X-ray spectra away from strong diffraction conditions. This is because of the Borrmann effect. Close to two-beam conditions, the Bloch waves interact strongly with the crystal planes and so X-ray emission is enhanced compared with kinematical conditions, thus negating the assumptions inherent in the Cliff-Lorimer equation, which assumes emission is constant with specimen tilt. However, we can make use of this phenomenon to locate which atoms lie on which crystal planes. The technique has the delightful (and wholly inappropriate) acronym ALCHEMI, which is a selective abbreviation of the expression 'atom location by channeling-enhanced microanalysis.'

ALCHEMI is a quantitative technique for identifying the crystallographic sites, distribution and types of substitutional impurities in crystals. The technique was first developed for the TEM by Spence (who, with archetypical antipodean humor, coined the acronym) and Taftø. Interestingly, channeling is also used for atom-site location in other analysis techniques (e.g., see Chu et al.).

The way to do ALCHEMI experimentally is to tilt your specimen to a strong two-beam condition and acquire a spectrum under strong channeling conditions, such that the Bloch wave is interacting strongly with a particular systematic row of atoms. You should choose the channeling orientation so that the specific crystal planes interacting strongly with the beam also contain the candidate impurity atom sites. So it helps a lot if you have some a priori ideas about where substitutional atoms are most likely to sit. This technique is therefore particularly well suited to layer structures. When the Bloch wave is maximized on a particular plane of atoms, the X-ray counts from the atoms in that plane will be highest. So start by finding the orientations 1 and 2 that give the most pronounced channeling effects for the atoms A and B, as shown schematically in Figure 35.10A. Usually a very small tilt is all that is necessary to get a different spectrum from the two planes.

If you are looking at two elements A and B and a substitutional element X then follow this procedure

- Measure X-ray intensities from each element in orientations 1 and 2.
- Then find a non-channeling orientation (3) where the electron intensity is uniform for both planes.

In this orientation we define the ratio k (NOT the Cliff-Lorimer factor) as

$$k = \frac{I_B}{I_A} \tag{35.36}$$

I_B is the number of X-ray counts from the element B in the non-channeling orientation. For the two channeling orientations 1 and 2, we define two parameters β and γ such that

$$\beta = \frac{I_B^{(1)}}{kI_A^{(1)}} \tag{35.37}$$

$$\gamma = \frac{I_B^{(2)}}{kI_A^{(2)}} \tag{35.38}$$

Now assuming we know from looking at the relative intensity changes in the spectra that the element X sits on specific sites, say it substitutes for atom B, then we define an intensity ratio term R such that

$$R = \frac{I_A^{(1)} I_X^{(2)}}{I_X^{(1)} I_A^{(2)}} \tag{35.39}$$

Then the fraction of atom X on B sites is given by

$$C_X = \frac{R-1}{R-1+\gamma-\beta R} \tag{35.40}$$

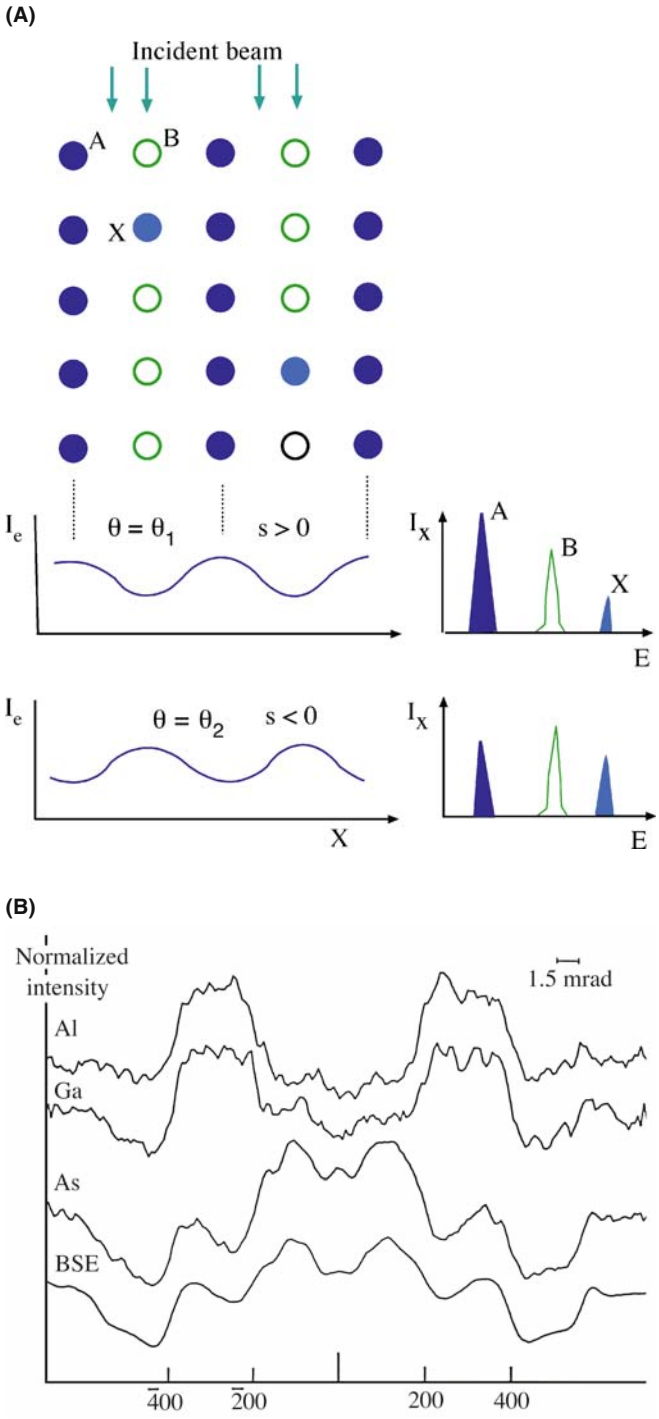

FIGURE 35.10. (A) ALCHEMI allows the determination of the site occupancy of atom X (light blue) in columns of atoms A (dark blue) and B (open circles). By tilting to **s** >0 and then **s** <0, the Bloch waves interact strongly with row A then row B giving different characteristic intensities, shown schematically in the spectra, from which the relative amounts of X in columns of A and B can be determined. (B) The Borrmann effect: the variation in the characteristic X-ray emission close to strong two-beam conditions as the beam is rocked across the 400 planes of GaAlAs. The X-rays from Al, which occupies Ga sites, follow the Ga emission variation while the As varies in an approximately complementary fashion. The BSE signal is inversely proportional to the amount of channeling so the As signal is strongest where the channeling is weakest.

Similar expressions can be generated for X atoms on A sites, but in fact the fraction of X atoms on A sites must be $1–C_X$.

As you see, ALCHEMI can give a direct measure of the occupation of substitutional sites. However, the intensity differences in different orientations are often quite small and you need good X-ray statistics to draw sound conclusions (counts, counts, and more counts!). This makes ALCHEMI difficult to apply if high spatial resolution is also desired because, as we shall see in the next chapter, the conditions to give the best spatial resolution also give the worst counting statistics. Figure 35.10B shows the variation in X-ray emission across a bend contour highlighting the Borrmann effect which is the basis of ALCHEMI. A comprehensive review has been given by Jones, who extends the discussion of the technique and develops it in depth in the companion text.

35.10 QUANTITATIVE X-RAY MAPPING

As we have discussed throughout the previous chapters, gathering X-ray maps rather than individual or lines of spectra makes a great deal of sense in terms of getting unbiased elemental-distribution information about your specimen. The major difficulty with moving from qualitative to quantitative mapping is the need for sufficient counts for quantification. As noted in Section 35.4.B above, we recommend acquiring 10,000 counts in a characteristic peak in order for reasonable quantification (i.e., with errors $\sim \pm$ 10% relative). A simple calculation will show how unrealistic this is if we are to acquire maps in a reasonable time. A minimum map to give a reasonable X-ray image is 128 $\times$ 128 pixels giving $>$ 16,000 total pixels. Even if we acquire for only 1 s/pixel (if we are lucky we will acquire a few tens of total counts rather than a few thousands), then we will be mapping for 4.5 hours minimum and more likely days if we wish to see hundreds or thousands of counts/pixel. As we've stated too often, such long times introduce specimen drift, damage, contamination, and operator boredom and so conspire to make life very difficult. While overnight mapping with lower-resolution EPMA systems (where the drift and stability requirements are much less stringent and the X-ray count rate is far greater) is indeed a common occurrence, STEMs are not yet stable enough to do this while retaining nanometer-level resolution.

Nevertheless, there has been significant progress in quantitative mapping, particularly with the use of 2–300 kV FEG instruments, the development of

higher solid angles of collection of X-rays, and general improvements in instrument design. So, as shown back in Figures 33.14 and 33.15, quantitative X-ray mapping is feasible. This process requires that the counts in the characteristic peak that is being mapped be integrated, subject to background subtraction, then processed via a Cliff-Lorimer or ζ-factor equation to turn the counts into composition. It is often best to exhibit the map as a color image because usually more than one element needs to be mapped or the composition changes need to be emphasized in which case overlays or side-by-side comparisons of the different maps permit easier understanding of the relative distributions of the various elements. Not surprisingly, quantitative mapping is improved by C_s correction since corrected probes have ~3–5× more current without loss of probe size. Thus the count rate is increased, or the acquisition time decreased, or both.

While it is certainly of interest to improve the stability of our TEM and XEDS systems and optimize the gathering of data over long periods of time, there are ways to minimize the limitations of low count rates and long acquisition times and this requires high-level computer control of the X-ray acquisition, implementation of spectrum imaging, or position-tagged spectrometry (check back in Sections 33.6.C and 33.6.D) and then manipulation of the resulting data cube using multivariate statistical analysis (MSA) to extract the maximum signal information and minimize the noise (which constitutes most of the signal in the channels in a spectrum acquired for a short period of time).

When this combination of SI and MSA is implemented, it is possible to gather spectra in as little as 100–500 ms/pixel giving mapping times of a few minutes to several tens of minutes for a 128 × 128 pixel image and it is equally feasible to contemplate larger maps. The SI/MSA combination is dealt with in great detail in the companion text. About the best that can be done with a modern C_s-corrected FEGSTEM, sophisticated data handling is shown in Figure 35.11 where segregation of trace elements to grain boundaries is mapped. A similar example was also shown back in Figure 33.15D which maps out differences in the composition of various small precipitates, a few nanometers in diameter. In Figure 35.11B, the data were acquired on a 300-keV STEM and the improvement in mapping quality obtained after MSA (Figure 35.11C) is clear. Addition of a C_s corrector to the STEM results in a further gain in spatial resolution, as shown in Figure 35.11D. This latter example of Zr segregating to a grain boundary in a Ni-base superalloy mapping reveals a typical enrichment of only ~1–2 atoms/nm^2 with a spatial resolution of ~0.5 nm!

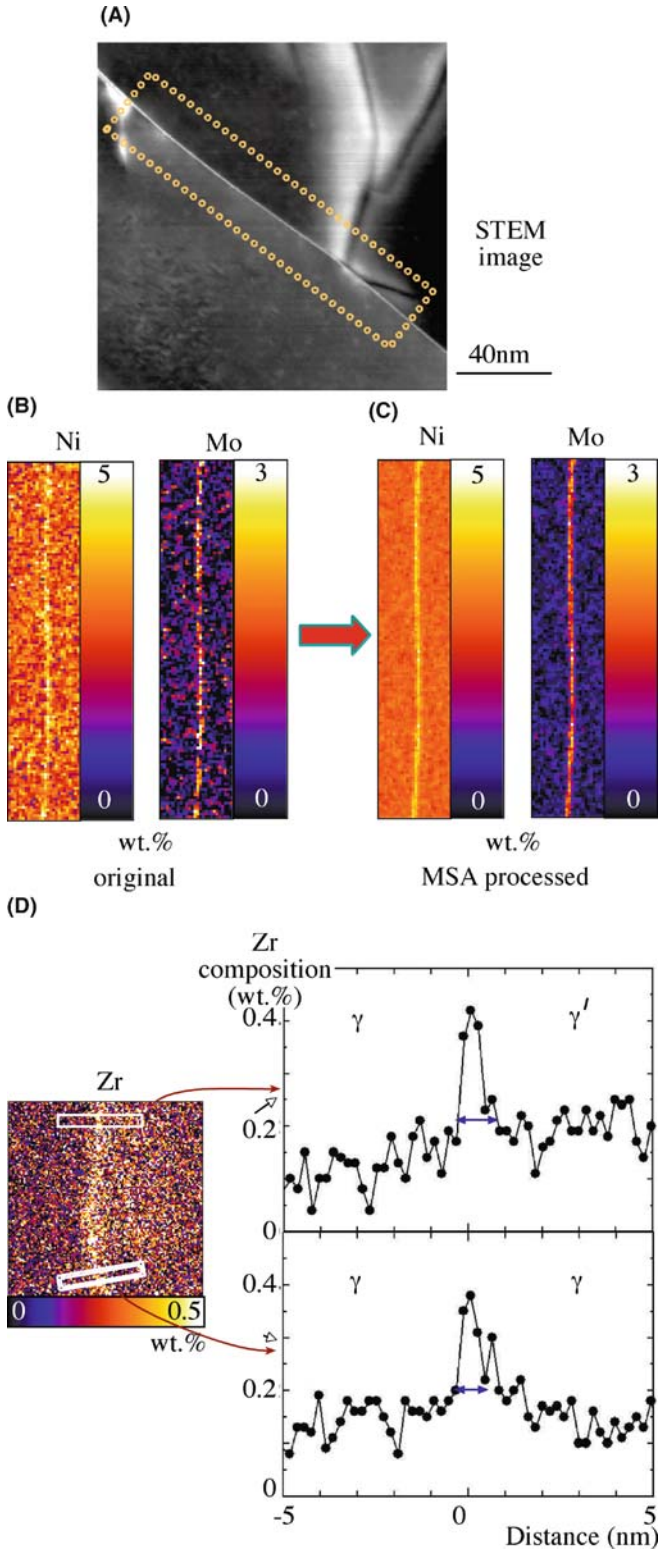

FIGURE 35.11. (A) STEM ADF image and (B) quantitative X-ray maps showing the segregation of trace amounts of Ni and Mo to grain boundaries in a low-alloy steel. (C) Applying MSA improves the quality of the maps. (D). Mapping the segregation of Zr to an interface in a Ni-base superalloy in a C_s-corrected STEM designed to give a 0.4-nm (FWTM) probe containing 0.5 nA. The Zr is present in the bulk alloy at ~0.04 wt% and without MSA processing could not be mapped. The composition profiles show that the Zr is localized to <1 nm at two different positions on the interface.

CHAPTER SUMMARY

The fact that much of this chapter is unchanged from the first edition sends a message that not much has changed in the last decade. This is unfortunate because, while quantitative analysis of spectra from thin foils can be straightforward, the standard Cliff-Lorimer approach has serious limitations. Most of the problems are overcome by the newer ζ-factor method, which is not yet commercially available but can be downloaded from the book web site (URL #2). Perhaps the greatest difficulty remains the need to know the specimen thickness in order to compensate for X-ray absorption and, again, the ζ-factor approach is invaluable in avoiding this. We can minimize absorption by making the thinnest possible specimens but then the number of X-ray counts may be so small that errors in the quantification are unacceptably large. The use of FEG sources, C_s correction, and improved TEM-EDS configurations with detector arrays to maximize the collection angle all help. With these latest advances, we can now perform quantitative X-ray mapping with a spatial resolution of a less than a nanometer and detection limits of a few atoms. There's much more about these exciting new aspects of quantitative analysis in the companion text.

GENERAL REFERENCES

Garratt-Reed, AJ and Bell, DC 2003 *Energy-Dispersive X-ray Analysis in the Electron Microscope* Bios (Royal Microsc. Soc.) Oxford UK.

Goodhew, PJ, Humphreys, FJ and Beanland, R 2001 *Electron Microscopy and Analysis* 3rd Ed. Taylor & Francis London. Instructive comparison of XEDS in SEM and TEM.

Goldstein, JI, Williams, DB and Cliff, G 1986 *Quantification of Energy Dispersive Spectra* in *Principles of Analytical Electron Microscopy* 155–217 Eds. DC Joy, AD Romig Jr. and JI Goldstein, Plenum Press New York. Introduction to many of the concepts in this chapter and the next one, including many worked examples.

Friel JJ and Lyman CE 2006 *X-ray Mapping in Electron-Beam Instruments* Microsc. Microanal. **12** 2–25. Detailed review of qualitative and quantitative mapping.

Jones, IP 1992 *Chemical Analysis Using Electron Beams* The Institute of Materials, London. The best source of examples of quantitative XEDS calculations.

Williams, DB and Goldstein, JI 1991 *Quantitative X-ray Microanalysis in the Analytical Electron Microscope in Electron Probe Quantitation* 371–398 Eds. KFJ Heinrich and DE Newbury Plenum Press New York. Derivations of the essential equations for thin-film quantification.

Zaluzec, NJ 1979 *Quantitative X-ray Microanalysis: Instrumental Considerations and Applications to Materials Science* in *Introduction to Analytical Electron Microscopy* Eds. JJ Hren JI Goldstein and DC Joy 121–167 Plenum Press NY. We've left this in so Nestor doesn't take us off his Web site.

CALCULATIONS

Anderson, IM, Bentley, J and Carter, CB 1995 *The Secondary Fluorescence Correction for X-Ray Microanalysis in the Analytical Electron Microscope* J. Microsc. **178** 226–239.

Bambynek, W, Crasemann, B, Fink, RW, Freund, HU, Mark, H, Swift, CD, Price, RE and Rao, PV *X-ray-fluorescence Yields, Auger and Coster-Kronig Transition Probabilities* 1972 Rev. Mod. Phys. **44** 716–813.

Cliff, G and Lorimer, GW 1975 *The Quantitative Analysis of Thin Specimens* J. Microsc. **103** 203–207. The original paper based on crushed mineral standards (all borrowed from the desk drawer of Pam Champness, Lorimer's wife, who is a well-known mineralogist).

Heinrich, KFJ 1986 *Mass Absorption Coefficients for Electron Probe Microanalysis* in *Proc. ICXOM-11* 67–77 Eds. J Brown and R Packwood University of Western Ontario Canada.

Powell, CJ 1976 *Evaluation of Formulas for Inner-shell Ionization Cross Sections* in *Use of Monte Carlo Calculations in Electron Probe Analysis and Scanning Electron Microscopy* 97–104 NBS Special Publication 460 Eds. KFJ Heinrich, DE Newbury and H Yakowitz U.S. Department of Commerce/NBS Washington DC.

Watanabe, M and Williams, DB 2006 *The Quantitative Analysis of Thin Specimens: a Review of Progress from the Cliff-Lorimer to the New ζ-Factor Methods* J. Microsc. **221** 89–109.

Williams, DB. Newbury, DE Goldstein, JI and Fiori, CE 1984 *On the Use of Ionization Cross Sections in Analytical Electron Microscopy* J. Microsc. **136** 209–218.

Schreiber, TP and Wims, AM 1981 *Quantitative Analysis of Thin Specimens in the TEM Using a $\phi(\rho z)$ Model* Ultramicrosc. **6** 323–334.

Schreiber, TP and Wims, AM 1982 *Relative Intensity Factors for K, L and M Shell X-ray Lines* X-ray Spectrometry **11** 42–45.
Larsen, RJ and Marx, ML 2001 *An Introduction to Mathematical Statistics and its Applications* 3rd Ed. Prentice Hall Upper Saddle River NJ.

CHANNELING

Chu, W-K, Mayer, JM and Nicolet, M-A 1978 *Backscattering Spectrometry* Academic Press Orlando.
Goldstein, JI, Newbury, DE, Echlin, P, Joy, DC, Romig, AD Jr, Lyman, C., Fiori, CE and Lifshin, E 2003 *Scanning Electron Microscopy and X-ray Microanalysis* 3rd Ed. Springer New York.

SOME HISTORY

Castaing, R 1951 *Application des Sondes Électroniques a une Méthode d'Analyse Ponctuelle Chimique et Cristallographique* Théses, Université de Paris ONERA Publication #55 Paris. A widely reproduced and historically significant publication.
Hillier, J and Baker, RF 1944 *Microanalysis by Means of Electrons* J. Appl. Phys. **15** 663–675.
Jones, IP 2002 *Determining the Locations of Chemical Species in Ordered Compounds; ALCHEMI* in *Advances in Imaging and Electron Physics* **125** 63–119.
Kramers, HA 1923 *On the Theory of X-ray Absorption and of the Continuous X- ray Spectrum* Phil. Mag. **46** 836–871.
Lorimer, GW, Al-Salman, SA and Cliff, G 1977 *The Quantitative Analysis of Thin Specimens: Effects of Absorption, Fluorescence and Beam Spreading* in *Developments in Electron Microscopy and Analysis* 369–371 Ed. DL Misell The Institute of Physics Bristol and London.
McGill, R. and Hubbard, FH 1981 *Quantitative Analysis with High Spatial Resolution* p30 Eds. GW Lorimer, MH Jacobs and P Doig The Metals Society London.
Reed, SJB 2005 *Electron Microprobe Analysis and Scanning Electron Microscopy in Geology* 2nd Ed. Cambridge University Press Cambridge UK.
Spence, JCH and Taftø, J 1983 *ALCHEMI - A New Technique for Locating Atoms in Small Crystals* J. Microsc. **130** 147–154.
Sprys, JW and Short, MA 1976 *Quantitative Elemental Analysis of 'Transparent' Particles in the TEM* Proc. 34th EMSA Meeting Ed. GW Bailey Claitors Baton Rouge LA 416–7
Statham PJ 2002 *Limitations to Accuracy in Extracting Characteristic Line Intensities From X-Ray Spectra* J. Research NIST **107** 531–546.
Wood, JE, Williams, DB and Goldstein, JI 1981 *Determination of Cliff-Lorimer k Factors for a Philips EM 400T* in *Quantitative Analysis with High Spatial Resolution* 24–30 Eds. GW Lorimer, MH Jacobs and P Doig The Metals Society London. k_{Fe} factors.

PROBLEMS WITH k_{ASi}

Goldstein, JI, Costley, JL, Lorimer, G, and Reed, SJB 1977 *Quantitative X-ray Microanalysis in the Electron Microscope SEM 1977* **1** 315–325 Ed. O Johari IITRI Chicago IL.
Graham, RJ and Steeds, JW 1984 *Determination of Cliff-Lorimer k Factors by Analysis of Crystallized Microdroplets* J. Microsc. **133** 275–280.
Sheridan, PJ 1989 *Determination of Experimental and Theoretical k_{ASi} Factors for a 200-kV Analytical Electron Microscope* J. Electr. Microsc. Tech. **11** 41–61.
Wood, JE, Williams, DB and Goldstein, JI 1984 *An Experimental and Theoretical Determination of k_{AFe} Factors for Quantitative X-ray Microanalysis in the Analytical Electron Microscope* J. Microsc. **133** 255–274.

URLS

1) mathworld.wolfram.com/Studentst-Distribution.html
2) http://www.TEMbook.com

SELF-ASSESSMENT QUESTIONS

Q35.1 Why do we have to correct the *k*-factor for absorption of X-rays?
Q35.2 Why is the fluorescence correction so small and generally ignored?
Q35.3 Why do we integrate only the K_α peak intensity rather than the $K_\alpha + K_\beta$ peaks if we can resolve them in the spectrum?
Q35.4 Why is the *k*-factor not a constant between different AEM-XEDS systems?
Q35.5 Why is the calculated *k*-factor generally inaccurate?
Q35.6 What's the largest contribution to the absorption correction and what does this tell you about ways to reduce your chance of having to do such?
Q35.7 What's the best way to minimize the errors in X-ray microanalysis?

Q35.8 What are the essential requirements for a good thin-foil standard and what does your list tell you about finding and selecting such standards?
Q35.9 What's the best way to measure the thickness of (a) your glass specimen, (b) your alloy foil, (c) your BN nanoparticle? (Hint: look ahead to Chapter 36.)
Q35.10 Why do quantitative analysis anyhow?
Q35.11 Why is it important to determine the errors in your quantitative analysis?
Q35.12 What is a typical ballpark quantification error in a simple binary (A–B) quantitative analysis?
Q35.13 What do you have to do to improve significantly on this error value?
Q35.14 When would you choose to use calculated *k*-factors rather than experimental ones?
Q35.15 When would you choose to determine your *k*-factors experimentally rather than calculate them?
Q35.16 List three ways to subtract the bremsstrahlung intensity from beneath the characteristic peaks in a spectrum.
Q35.17 Distinguish bremsstrahlung, continuum, and background X-rays.
Q35.18 What does ALCHEMI stand for and why is it anything but alchemy?
Q35.19 Why do we typically use wt% rather than at.% in X-ray microanalysis?
Q35.20 Why is it best to have as thin a window as possible on your XEDS detector but why is it generally impractical to have no window at all?

TEXT-SPECIFIC QUESTIONS

T35.1 If *k*-factors are not constants, what is the use of tables of *k*-factors, such as Tables 35.1 and 35.2?
T35.2 What are 'residuals' in the filtered spectra in Figure 35.6 and why are they useful?
T35.3 Distinguish top-hat apertures and top-hat filters and explain why both are useful in AEM-XEDS.
T35.4 Why would you use the two-window method of background subtraction as shown in Figure 35.5 rather than the one-window method in Figure 35.4?
T35.5 Why does the background intensity go to zero in Figure 35.4 and what experimental and instrumental factors affect the energy at which it goes to zero?
T35.6 Why do the values of the *k*-factors shown in Figure 35.7 decrease with decreasing atomic number and then increase again? (Hint: there's a good physics explanation for both of these trends.)
T35.7 Copy Figure 35.8 and extrapolate the three lines to lower thickness. At what value of thickness do they converge and why is this the case?
T35.8 Give three limitations to the *k*-factor approach that are overcome by the ζ-factor method?
T35.9 What is the single most cautionary lesson you can gain from Figure 35.10A?
T35.10 Why, in the AEM, can we measure elemental segregation phenomena generated in materials at lower temperatures compared with EPMA experiments? (Hint: think abut diffusion kinetics.)
T35.11 You have standard thin foils of Fe_2O_3, NiO, Ni_3Al, $CuSO_4$. Explain how you would determine *k*-factors for analysis of (a) FeS, (b) NiAl, (c) Al_2O_3, and (d) Al-Cu solid solution. List any specific concerns you may have with your determinations.
T35.12 Using Table 35.1, calculate reasonable first approximations for the *k*-factors for (a) Mn-Cr, (b) Mg-Al, and (c) Al-Cu. State any assumptions you make in your calculations.
T35.13 Using the DTSA software, practice generating X-ray spectra for different elements and compounds at different accelerating voltages (e.g., 100–300 kV) and different take-off angles (e.g., $\alpha = 20^\circ, 60^\circ$). Observe the differences in the background and characteristic spectra as a function of kV and α. Use the background-subtraction options to measure peak intensities and run practice quantifications.
T35.14 Using DTSA run quantification routines for a single binary specimen of your choice, but select a range of ionization cross sections with which to calculate a *k*-factor and compare the range of answers that you get for your *k*-factor and your quantification. What does this tell you about the limitations of calculated *k*-factors?
T35.15 Calculate the absorption correction factor (ACF) for Fe-10 wt% Al foils 10, 100, and 300 nm thick for different take-off angles of 20° and 70°. Then, evaluate the specimen thickness necessary to meet the thin-film criterion (> 10% absorption). Use 6.61 g/cm^3 for the specimen density and following data for the mass-absorption coefficients for Fe K_α, Fe L_α, and Al K_α lines (Heinrich 1986). If you wish, after completing the manual calculation compare your result with DTSA calculation of the same correction. (courtesy M. Watanabe)

	Mass-absorption coefficient (cm^2/g)		
Absorber	Fe K_α	Fe L_α	Al K_α
Fe	71.1	2,157	3,626
Al	96.5	2,936	397.5